

The Family of Ferrocene-Stabilized Silylium Ions: Synthesis, ^{29}Si NMR Characterization, Lewis Acidity, Substituent Scrambling, and Quantum-Chemical Analyses

Kristine Mütter,^[a, b] Peter Hrobárik,^{*,[a, c]} Veronika Hrobáriková,^[a, d]
Martin Kaupp,^{*,[a]} and Martin Oestreich^{*,[a, b]}

Abstract: The purpose of this systematic experimental and theoretical study is to deeply understand the unique bonding situation in ferrocene-stabilized silylium ions as a function of the substituents at the silicon atom and to learn about the structure parameters that determine the ^{29}Si NMR chemical shift and electrophilicity of these strong Lewis acids. For this, ten new members of the family of ferrocene-stabilized silicon cations were prepared by a hydride abstraction reaction from silanes with the trityl cation and characterized by multinuclear ^1H and ^{29}Si NMR spectroscopy. A closer look at the NMR spectra revealed that additional minor sets of signals were not impurities but silylium ions with substitution patterns different from that of

the initially formed cation. Careful assignment of these signals furnished experimental proof that sterically less hindered silylium ions are capable of exchanging substituents with unreacted silane precursors. Density functional theory calculations provided mechanistic insight into that substituent transfer in which the migrating group is exchanged between two silicon fragments in a concerted process involving a ferrocene-bridged intermediate. Moreover, the quantum-chemical analysis of the ^{29}Si NMR chemical shifts revealed

Keywords: density functional theory • donor–acceptor interactions • Lewis acids • silylium ions • substituent scrambling

a linear relationship between $\delta(^{29}\text{Si})$ values and the $\text{Fe}\cdots\text{Si}$ distance for subsets of silicon cations. An electron localization function and electron localization indicator analysis shows a three-center two-electron bonding attractor between the iron, silicon, and C'_{ipso} atoms, clearly distinguishing the silicon cations from the corresponding carbenium ions and boranes. Correlations between ^{29}Si NMR chemical shifts and Lewis acidity, evaluated in terms of fluoride ion affinities, are seen only for subsets of silylium ions, sometimes with non-intuitive trends, indicating a complicated interplay of steric and electronic effects on the degree of the $\text{Fe}\cdots\text{Si}$ interaction.

Introduction

The pronounced electron deficiency of tricoordinate silicon cations (silylium, silylenium, or silicenium ions) coerces these strong Lewis acids to seek stabilization by electron density in their proximity.^[1] Even π -basic arene solvents^[2] and weakly σ -coordinating counteranions, such as Reed's $[\text{HCB}_{11}\text{H}_5\text{Br}_6]^-$ anion,^[3] are not innocent and coordinate to the silicon atom. The $\text{Si}-\text{H}$ bond of a remaining precursor will also interact with the empty orbital at the silicon atom, forming a three-center two-electron ($3c2e$) $[\text{Si}\cdots\text{H}\cdots\text{Si}]^+$ bridge.^[4] These intermolecular Lewis acid–base interactions had thwarted the isolation of the free cation,^[2–4] and it was steric bulk around the trigonal planar silicon atom that eventually resulted in success ($\text{Mes}_3\text{Si}^+[\text{B}(\text{C}_6\text{F}_5)_3]^-$ with ^{29}Si NMR (C_6D_6): $\delta = 225.5$ ppm).^[5]

Conversely, the same effects were deliberately utilized to intramolecularly stabilize silylium ions, and several beautiful molecules were designed in which the Lewis basic group is cleverly positioned to allow for controlled taming of the Lewis acidity (Figure 1). An elegant implementation using an alkene π donor is seen in the preparation of a silicon var-

[a] K. Mütter, Dr. P. Hrobárik, Dr. V. Hrobáriková, Prof. Dr. M. Kaupp, Prof. Dr. M. Oestreich
Institut für Chemie, Technische Universität Berlin
Strasse des 17. Juni 115, 10623 Berlin (Germany)
E-mail: martin.kaupp@tu-berlin.de
martin.oestreich@tu-berlin.de

[b] K. Mütter, Prof. Dr. M. Oestreich
Organisch-Chemisches Institut
Westfälische Wilhelms-Universität Münster
Corrensstrasse 40, 48149 Münster (Germany)

[c] Dr. P. Hrobárik
Institute of Inorganic Chemistry, Slovak Academy of Sciences
Dúbravská cesta 9, 84536 Bratislava (Slovakia)
E-mail: peter.hrobarik@savba.sk

[d] Dr. V. Hrobáriková
Department of Organic Chemistry
Faculty of Natural Sciences, Comenius University
Mlynská dolina, 84215 Bratislava (Slovakia)

Supporting information for this article is available on the WWW under <http://dx.doi.org/10.1002/chem.201302885>.

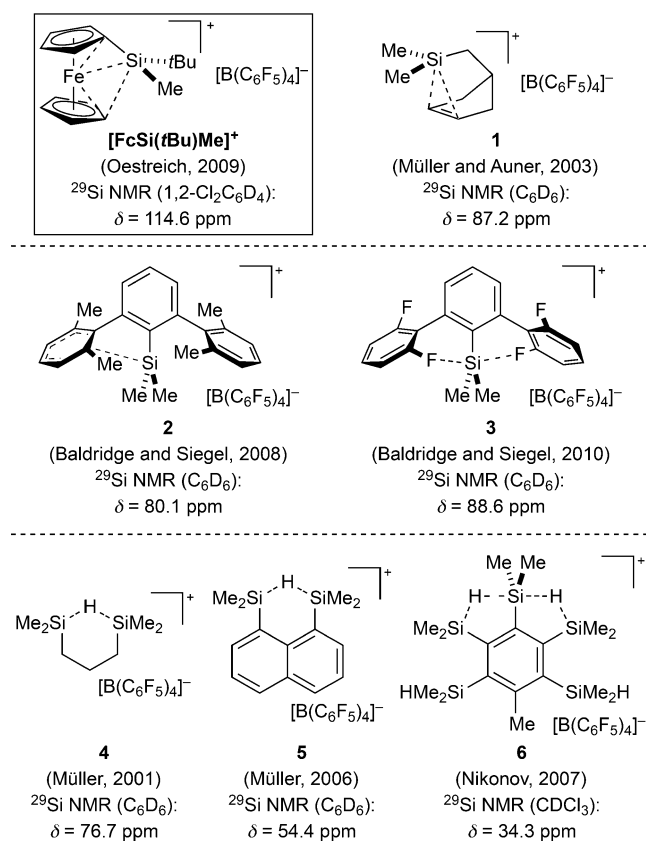


Figure 1. Selected intramolecularly stabilized silylium ions with ^{29}Si NMR chemical shifts.

iant of the norbornyl cation (**1**; Figure 1, upper right).^[6] The Baldrige/Siegel team recently introduced a new class of silicon cations with various terphenyl substituents. The roof-like structure not only provides kinetic stabilization through steric shielding of the silicon cation but also thermodynamic stabilization through fast oscillation of the cationic silicon atom between the π systems of the flanking arenes (**2**; Figure 1, middle left).^[7] A similar effect was achieved by interaction with neutral halogen atoms (**3**, middle right).^[8] A conceptually novel approach to intramolecular silicon cation stabilization was presented by Müller (**4** and **5**, lower left and middle).^[9] Intramolecular 3c2e $[\text{Si}\cdots\text{H}\cdots\text{Si}]^+$ bridges delocalize the positive charge in such a way that steric shielding is not required anymore. Several congeners are known today (not shown),^[1] and the structure of **6** (Figure 1, lower right) is particularly noteworthy.^[10] In all these cases, coordination of neither solvent nor counteranion is an issue. Incorporation of the silicon atom into cyclic π -conjugated systems is another general strategy to stabilize silylium ions in their free form (not shown).^[11]

We follow a different approach to intramolecular stabilization of the tricoordinate silicon cation. The well-understood stabilization of the isoelectronic carbenium ions^[12] and related boranes^[13] by an electron-rich metallocenyl group attached to it stimulated us a few years ago to consider the related metallocene-substituted silylium ions. The idea of gen-

erating ferrocene (Fc) stabilized silylium ions had not been new at that time as there were reports by Corey^[14] and Manners^[15] of anion- and solvent-coordinated systems, respectively. A purely intramolecularly stabilized, that is, free, α -ferrocenylsilylium ion had, however, been elusive until we accomplished its preparation and spectroscopic characterization ($[\text{FcSi}(\text{tBu})\text{Me}]^+$; Figure 1, upper left).^[16]

We were recently able to determine the molecular structure and the bonding situation of our ferrocene-stabilized silicon cation $[\text{FcSi}(\text{tBu})\text{Me}]^+$ by crystal structure analysis and quantum-chemical calculations (Figure 2, upper).^[17] The

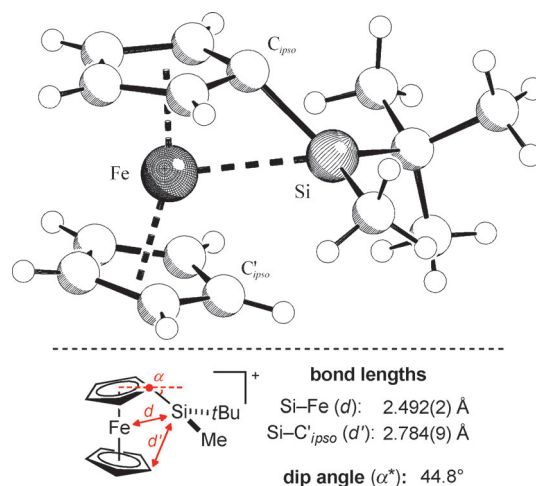


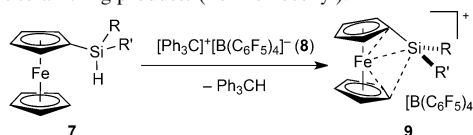
Figure 2. Molecular structure of our ferrocene-stabilized silylium ion $[\text{FcSi}(\text{tBu})\text{Me}]^+$ with relevant data (boranate counter anion $[\text{B}_{12}\text{Cl}_{12}]^{2-}$ is omitted for clarity).

strong interaction between the cationic silicon atom and the ferrocene backbone is reflected in short distances between the silicon atom and the iron atom ($d = 2.492$ Å) as well as the *ipso* carbon atom of the lower Cp ring ($d' = 2.784$ Å). To accommodate these bonds, a large dip angle ($\alpha^* = 44.8^\circ$) of the silicon atom out of the plane of the upper Cp ligand results (Figure 2, lower). For comparison, that dip angle is substantially smaller ($\alpha^* = 20.7^\circ$) in the phenyl-substituted α -ferrocenylcarbenium ion, in which the positive charge is partially delocalized into the upper Cp ligand, now showing fulvene character.^[12,18]

Based on our previous work on a single member, we introduce here a large family of ferrocene-stabilized silylium ions bearing both aryl (including additional ferrocenyl) and alkyl substituents at the cationic silicon atom. Our account comprises full spectroscopic characterization with experimental ^{29}Si NMR chemical shifts confirmed by quantum-chemical calculations. A detailed analysis of chemical shifts, stability and Lewis acidity, and their correlation with structural and electronic factors is provided. Moreover, careful analysis of ^1H and ^{29}Si NMR spectra reveals scrambling of substituents at the silicon atom, and it is possible to assign the additional sets of signals to silicon cations with redistributed substitution patterns. Supported by quantum-chemical

calculations, we present a concerted reaction mechanism for the substituent exchange between the initially formed silylium ion and remaining silane precursor.

Table 1. NMR spectroscopic data of all ferrocenylsilanes **7a–7k** and silylium ions **9a–9k** as well as an overview of observed substituent scrambling products (Fc = ferrocenyl).



Computational Methods

The ground-state structures of all systems under investigation were fully optimized (without counterion) at the PBE0 level of theory,^[19] including an atom-pairwise correction for dispersion forces (Grimme's D3 model)^[20] and employing def2-TZVPP basis sets^[21] for all atoms. For comparative purposes, the selected structures were also optimized at the PBE0/def2-TZVPP level without dispersion corrections and at the TPSS-D3/def2-TZVPP^[22] level used in a previous study.^[17] The optimized structures were characterized as true minima on the potential energy hypersurface by harmonic vibrational frequency analyses. Transition-state structures were located as follows: initially detailed geometry scans between the two local minima were performed. The maxima obtained were consequently used as starting points of full transition-state optimizations. The transition states were verified by subsequent harmonic vibrational frequency calculations. All these calculations were carried out with Turbomole.^[23] Calculations of NMR nuclear shieldings were performed in the Gaussian09 program package^[24] using gauge-including atomic orbitals (GIAO)^[25] at the PBE0 level, employing modified TZVP all-electron basis set of (15s11p6d)/[9s7p4d] quality for iron and Huzinaga–Kutzelnigg-type IGLO-III basis set for all other atoms.^[26,27] The calculated ¹H and ²⁹Si NMR shieldings were converted to chemical shifts (δ in ppm) relative to the shieldings of tetramethylsilane (TMS). In these calculations, bulk solvent effects were simulated by means of the integral equation formalism of the polarizable continuum model (IEF-PCM)^[28] whereas a conductor-like screening solvation model (COSMO)^[29] was employed in structure optimizations and energy evaluations. In both cases, 1,2-Cl₂C₆H₄ with $\epsilon_r = 9.8$ was considered as the solvent. The structures of the selected silylium ions remained essentially unaffected when a continuum solvation model was applied in the optimization procedure (this does not hold for the energies though) and, therefore, only the gas-phase structures were used throughout this work. The wave functions were analyzed by means of the electron localization function (ELF)^[30] and the electron localization indicator (ELI-D),^[31] respectively, using the DGrid program^[32] with grids using ten points per Bohr. Mayer bond orders^[33] were calculated using the program BORDER.^[34] The results of ELF and ELI-D analyses were visualized by using the ParaView program.^[35]

Results and Discussion

Silylium ion precursors; silane preparation: Silylium ions are commonly prepared by hydride abstraction from the corresponding silane precursor using [Ph₃C]⁺[B(C₆F₅)₄]⁻ (**8**).^[36] For the generation of ferrocene-stabilized silicon cations, we prepared a series of differently substituted ferrocenylsilanes **7a–7k** (Table 1). Monoferrocenylsilanes **7a–7f** and **7j** were

synthesized in good yields (49–91 %) by monolithiation of ferrocene using *t*BuLi and a catalytic amount of KO*t*Bu^[37,38] and subsequent treatment with an appropriate monochlorosilane. Ferrocenylmethylphenylsilane (**7g**) was obtained in a slightly lower yield of 48 % from monolithiated ferrocene and dichloromethylphenylsilane followed by reduction with LiAlH₄. Using an excess of monolithiated ferrocene and the corresponding dichlorosilane, diferrocenylsilanes **7i** and **7k** were accessible in the same way in 66 and 76 % yield, respectively. For bulkier substituents (*i*Pr and *t*Bu), the synthesis of diferrocenylsilanes was not successful, probably due to the steric bulk around the silicon atom. Nevertheless, we succeeded in the preparation of the sterically very hindered triferrocenylsilane (**7h**) in a moderate yield of 31 %.^[39]

The NMR spectroscopic characterization of ferrocenylsilanes **7a–7k** was carried out in C₆D₆. Of particular interest are the chemical shifts of the Si–H functionality in the ¹H and ²⁹Si NMR spectra (Table 1, columns 5 and 6). The hydride shifts are observed in the range of $\delta = 4.16$ –5.78 ppm depending on the substitution pattern at the silicon atom. For dialkyl-substituted ferrocenylsilanes **7a–7e** a shift between $\delta = 4.16$ –4.69 ppm is obtained, whereas mono- and diaryl-substituted silanes **7f–7k** lead to a more deshielded signal between $\delta = 4.83$ –5.78 ppm. ²⁹Si NMR spectroscopy shows an opposite trend: more aryl substituents at the silicon atom result in a low-frequency shifted signal.

Silylium ions: With these ferrocenylsilanes (**7a–7k**) in hand, we were able to synthesize a new family of ferrocene-stabilized silicon cations.^[40] All silylium ions **9a–9k** were rapidly generated from the corresponding silanes at room tempera-

Entry	Silane precursor ^[a]			Silylium ion ^[b]		Substituent scrambling products		
	R	R'	Cmpd	¹ H NMR Si–H [ppm]	²⁹ Si NMR [ppm]		Cmpd	²⁹ Si NMR [ppm]
1	<i>t</i> Bu	<i>t</i> Bu	7a	4.16	7.6 ^[c]	9a	120.3 ^[d] /120.9 ^[e]	–
2	<i>i</i> Pr	<i>i</i> Pr	7b	4.29	1.4 ^[c]	9b	114.1 ^[d] /114.7 ^[e]	–
3	<i>t</i> Bu	Me	7c	4.36	–2.7 ^[c]	9c	113.9 ^[d] /114.4 ^[e]	9l ^[f]
4	<i>i</i> Pr	Me	7d	4.46	–7.6 ^[c]	9d	113.5 ^[d] /113.4 ^[e]	9m ^[g]
5	Me	Me	7e	4.69	–18.8 ^[c]	9e	111.0 ^[d] /110.7 ^[e]	9i
6	Ph	<i>t</i> Bu	7f	4.83	–0.4 ^[c]	9f	98.8 ^[d] /98.6 ^[e]	9l ^[f]
7	Ph	Me	7g	5.18	–18.5 ^[c]	9g	93.8 ^[e]	9e, 9i, 9j, 9k
8	Fc	Fc	7h	5.73	–21.4 ^[c]	9h	91.3 ^[d] /91.3 ^[e]	–
9	Fc	Me	7i	5.21	–20.5 ^[c]	9i	88.5 ^[d] /88.3 ^[e]	9h
10	Ph	Ph	7j	5.72	–17.7 ^[c]	9j	81.4 ^[d] /81.0 ^[e]	9k
11	Fc	Ph	7k	5.78	–18.3 ^[c]	9k	77.5 ^[d] /77.4 ^[e]	9h

[a] NMR data for all silanes were measured in C₆D₆. [b] Silylium ions were generated according to general procedure 2 (GP 2, see the Experimental Section) as a solution (175–236 μ m) in 1,2-Cl₂C₆H₄ and directly subjected to NMR spectroscopic analysis. [c] ²⁹Si DEPT NMR spectroscopy. [d] ¹H, ²⁹Si HMQC NMR spectroscopy. [e] ²⁹Si NMR spectroscopy. [f] Silylium ion **9l** (R = Fc, R' = *t*Bu) was only obtained from substituent scrambling; ²⁹Si NMR: $\delta = 104.5$ ppm. [g] Silylium ion **9m** (R = Fc, R' = *i*Pr) was only obtained from substituent scrambling; ²⁹Si NMR: $\delta = 100.4$ ppm.

ture using Corey's hydride abstraction reaction (Table 1, 7→9).^[36] The samples were prepared in 1,2-Cl₂C₆D₄ and directly subjected to multinuclear NMR spectroscopy.

Structure, bonding, and stabilization energies: An unprecedented bonding motif in ferrocene-stabilized silylium ions had already been indicated in the previous structural characterization of the first member of this series, [FcSi(*t*Bu)Me]⁺[B(C₆F₅)₄]⁻, on the basis of localized molecular orbitals (LMOs).^[17] Specifically, the extreme dip angle of the silicon atom toward the iron center was rationalized by two 3c2e

bonds through participation of both the upper and the lower Cp rings of the ferrocene sandwich structure. The unusual bonding situation is apparent also in the Mayer bond orders (MBO) between the silicon atom and its neighbors (Table 2 and Table 3). Furthermore, the Fe⋯Si distance in [FcSi(*t*Bu)Me]⁺ determined experimentally and computationally, *d*(Fe⋯Si) ≈ 2.49 Å, is close to the sum of iron and silicon single-bond covalent radii (1.16 + 1.16 = 2.32 Å).^[41] We note in passing that the Fe⋯Si distances and dip angles are closely correlated in the studied series (Figure S1 in the Supporting Information).

In an attempt to analyze the nature of the interactions between the silicon and iron atoms and the Cp ligands further, we examined here the real-space functions ELF (electron localization function) and ELI-D (electron localizability indicator). The results of the ELI-D analysis on silicon cation [FcSiMe₂]⁺ and carbocation [FcCMe₂]⁺ are shown in Figure 3 (the very similar ELF picture is given in Figure S2 in the Supporting Information; see also Table S1 for the values of ELF and ELI-D attractors). A three-center-bonding attractor between iron, silicon and the C'_{ipso} atom of the lower Cp ring can be clearly identified. The presence of this attractor clearly distinguishes the ferrocene-stabilized silylium ions from the corresponding carbenium ions, consistent with the large dip angle between

Table 2. Computed interatomic distances, dip angles, stabilization energies, and Mayer bond orders (MBO) in ferrocene-stabilized electrophiles (Scheme 1).^[a]

System ^[b]	Distances				MBO		
	<i>d</i> (Fe⋯E) [Å]	<i>d</i> (E⋯C' _{ipso}) [Å]	α^* [°]	ΔE_r [kJ mol ⁻¹] ^[c]	ΔE_{stab} [kJ mol ⁻¹] ^[d]	Fe⋯E	E⋯C' _{ipso}
FcBMe ₂	2.921	2.888	13.4	-26.1	-3.5	0.09	0.01
FcAlMe ₂	2.989	3.294	32.5	-32.1	-12.5	0.12	0.07
[FcCMe ₂] ⁺	2.513	3.061	29.1	-85.8	-16.9	0.27	0.03
[FcSiMe ₂] ⁺	2.462	2.596	45.0	-106.8	-58.9	0.44	0.26
[FcGeMe ₂] ⁺	2.580	2.718	43.0	-89.6	-45.6	0.34	0.20
[FcSnMe ₂] ⁺	2.774	2.823	41.6	-79.1	-40.9	0.31	0.17
[FcPbMe ₂] ⁺	2.942	2.987	37.3	-58.7	-24.8	0.26	0.15

[a] PBE0-D3/def2-TZVPP results (see the Computational Methods for more detail). [b] E atoms are given in bold. [c] See Scheme 1 for the reaction; R = R' = Me. [d] Stabilization energy calculated as a difference between energies of the fully optimized structure and corresponding structure optimized with a fixed dip angle $\alpha^* = 0.0^\circ$.

Table 3. Optimized structural parameters, relative stabilities (ΔE_r and ΔE_{stab}), fluoride ion affinities (FIA), Mayer bond orders (MBO), and computed ²⁹Si NMR chemical shifts in a series of ferrocene-stabilized silylium ions [FcSiR(R')]⁺.^[a,b]

R	R'	<i>d</i> (Fe⋯Si) [Å]	<i>d</i> (Si⋯C' _{ipso}) [Å]	α^* [°]	ΔE_r [kJ mol ⁻¹]	ΔE_{stab} [kJ mol ⁻¹]	FIA [kJ mol ⁻¹]	MBO	$\delta(^{29}\text{Si})$ [ppm] ^[c]	
								Fe⋯Si	Si⋯C' _{ipso}	
Me	Me	2.462	2.596	45.0	-106.8	-58.9	816.6	0.436	0.255	114.7
<i>i</i> Pr	Me	2.477	2.604	44.6	-105.0	-56.1	814.8	0.427	0.279	116.3
<i>t</i> Bu	Me	2.487	2.616	44.2	-104.9	-54.3	816.0	0.420	0.293	115.9
<i>i</i> Pr	<i>i</i> Pr	2.491	2.603	44.1	-106.0	-52.0	809.2	0.425	0.299	118.3
<i>t</i> Bu	<i>t</i> Bu	2.539	2.706	42.3	-96.6	-41.7	818.3	0.423	0.285	125.3
Ph	Me	2.488	2.640	44.1	-90.5	-45.6	806.7	0.449	0.264	95.2
Ph	<i>t</i> Bu	2.493	2.606	44.1	-95.8	-50.4	810.0	0.440	0.273	98.7
Mes	Me	2.593	2.865	40.3	-59.6	-18.7	815.1	0.416	0.220	114.1
Mes	<i>t</i> Bu	2.688	3.018	36.7	-62.2	-19.2	802.0	0.390	0.200	128.7
Ph	Ph	2.515	2.688	43.2	-77.1	-36.6	798.8	0.457	0.281	85.8
4-Tolyl	4-Tolyl	2.535	2.706	42.4	-69.7	-31.3	786.7	0.444	0.270	86.6
3,5-Xylyl	3,5-Xylyl	2.534	2.702	42.5	-71.5	-33.0	783.0	0.449	0.277	86.8
2-Naphthyl	2-Naphthyl	2.528	2.692	42.8	-67.4	-30.9	792.1	0.450	0.272	87.8
1-Naphthyl	1-Naphthyl	2.599	2.866	40.1	-58.2	-21.5	810.2	0.456	0.212	88.7
Mes	Mes	2.730	3.076	35.6	-38.2	-6.7	786.3	0.429	0.162	108.1
<i>p</i> -NMe ₂ -Ph	<i>p</i> -NMe ₂ -Ph	2.656	2.821	37.9	-43.4	-11.6	744.3	0.360	0.210	92.9
<i>p</i> -OMe-Ph	<i>p</i> -OMe-Ph	2.569	2.734	41.2	-58.2	-22.7	775.1	0.418	0.255	86.8
<i>p</i> -CN-Ph	<i>p</i> -CN-Ph	2.472	2.645	44.8	-89.4	-44.2	852.4	0.488	0.305	81.4
<i>p</i> -NO ₂ -Ph	<i>p</i> -NO ₂ -Ph	2.463	2.637	45.1	-93.7	-47.2	856.3	0.496	0.308	81.0
Fc	Me	2.585	2.732	40.4	-38.5	-39.8	789.9	0.384	0.239	89.1
Fc	<i>i</i> Pr	2.545	2.682	42.0	-37.3	-38.9	785.4	0.383	0.270	102.3
Fc	<i>t</i> Bu	2.559	2.706	41.5	-27.9	-35.0	792.2	0.400	0.297	107.7
Fc	Ph	2.627	2.777	38.8	-37.0	-31.4	784.0	0.444	0.276	73.6
Fc ^[d]	Fc ^[d]	2.589	2.759	40.4	-27.9	-24.3	779.4	0.403	0.241	99.2
Fc ^[d]	Fc ^[d]	2.615	2.762	39.3	-27.0	-21.1	780.3	0.409	0.245	87.7

[a] PBE0-D3/def2-TZVPP results in the gas-phase if not stated otherwise (see the Computational Methods for more detail). [b] Only structure parameters corresponding to the primary Lewis acid–base Fe⋯Si interactions are given here (see Table 4 for secondary through-space interactions in compounds containing more than one Fe unit). [c] PBE0/IGLO-III/PBE0-D3/def2-TZVPP results using an IEF-PCM solvation model. [d] Data reported for the two minima found for [FcSiFc]⁺.

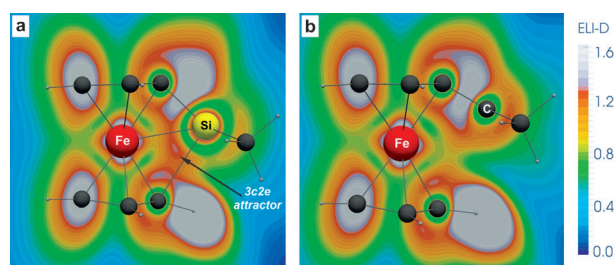
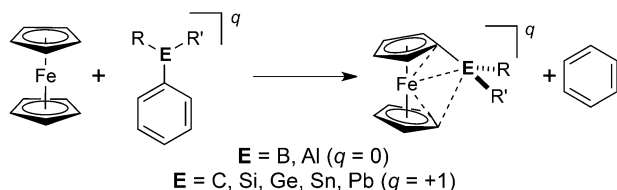


Figure 3. ELI-D analysis of bonding in the ferrocene-stabilized a) silicon cation $[\text{FcSiMe}_2]^+$, and b) in the corresponding carbocation $[\text{FcCMe}_2]^+$. The selected planes include the iron (in red), C'_{ipso} and positively charged silicon (in yellow) or carbon (in dark grey) atoms.

the $\text{Si}-\text{C}'_{\text{ipso}}$ bond and the upper Cp plane. Going down in the periodic table, a corresponding bonding attractor is also found in the analogous ferrocene-stabilized germanium(IV) cation but not in the tin(IV) and lead(IV) congeners (Figure S3 in the Supporting Information). A second $3c2e$ bond between iron, silicon, and C'_{ipso} of the upper ring is not evident from the ELF and ELI-D analysis. However, the presence of such an interaction cannot be excluded as the corresponding attractor could overlap with that of the $\text{Si}-\text{C}'_{\text{ipso}}$ bond. The moderate Mayer bond orders for a $\text{Fe}\cdots\text{E}^+$ pair in $[\text{FcE}(\text{Me}_2)]^+$ ions (Table 2) as well as the non-negligible dip angle and stabilization energies ΔE_{stab} in all these systems (see below) hint at the attractive intramolecular donor-acceptor interaction between the electrophilic center and the metallocene backbone.

To quantify the strength of the ferrocene-electrophile interaction, we calculated the energy of the isodesmic reaction, ΔE_r , where a Ph moiety in the $[\text{PhER}(\text{R}')^q]$ series ($\text{E} = \text{B}, \text{Al}/\text{C}, \text{Si}, \text{Ge}, \text{Sn}, \text{Pb}$; $q = 0/+1$; R and R' stand for alkyl or aryl) is replaced by an Fc unit (Scheme 1). Note that ΔE_r contains also contributions from stabilization due to a somewhat stronger electron-donating effect of a metallocene backbone compared to the Ph substituent, in addition to the possible presence of a direct $\text{Fe}\cdots\text{E}$ donor-acceptor interaction. For this reason, we calculated additionally a stabilization energy ΔE_{stab} as a difference between the energies of



Scheme 1. Isodesmic reaction used to determine the stabilization energy (ΔE_r) due to the metallocene-electrophile interaction.

the fully optimized silylium ions and the corresponding partially optimized structures with a fixed dip angle $\alpha^* = 0.0^\circ$. In case of the multiply ferrocene-stabilized systems, ΔE_{stab} in Table 3 refers to only the primary interaction obtained indirectly by fixing α^* to 0.0° for all Fc moieties and subtracting the energy of the secondary interaction(s) given in Table 4.

Among the group 14 elements, the largest stabilization is indeed obtained for the silylium system. A decrease in the stabilization energy with increasing atomic number from silicon to lead is accompanied by decreased dip angles α^* (from 45.0° to 37.3°). The most pronounced stabilization of silylium ion can be explained by: 1) easier bending of the $\text{C}'_{\text{ipso}}-\text{Si}$ bond out of the Cp ring plane compared to the car-

Table 4. Computed interatomic distances, dip angles, and stabilization energies of the secondary through-space interactions in silylium ions $[\text{FcSiR}(\text{R}')^q]^+$ with more than one Fc unit.^[a]

R	R'	Unit B				Unit C				
		$d(\text{Si}\cdots\text{Fe})$ [Å]	$d(\text{Si}\cdots\text{C}'_{\text{ipso}})$ [Å]	$d(\text{Si}-\text{C}'_{\text{ipso}})$ [Å]	α^* [°]	$d(\text{Si}\cdots\text{Fe})$ [Å]	$d(\text{Si}\cdots\text{C}'_{\text{ipso}})$ [Å]	$d(\text{Si}-\text{C}'_{\text{ipso}})$ [Å]	α^* [°]	ΔE_{stab} [kJ mol ⁻¹] ^[b]
Fc	Me	3.093	3.324	1.800	18.4	–	–	–	–	4.5
Fc	<i>i</i> Pr	3.295	3.605	1.813	8.6	–	–	–	–	1.5
Fc	<i>t</i> Bu	3.340	3.656	1.825	6.4	–	–	–	–	1.0
Fc	Ph	3.065	3.285	1.801	19.8	–	–	–	–	4.4
Fc ^[c]	Fc ^[c]	3.332	3.661	1.809	6.2	3.458	3.907	1.819	1.7	1.4
Fc ^[c]	Fc ^[c]	3.135	3.393	1.804	16.6	3.521	4.056	1.822	4.5	4.6

[a] PBE0-D3/def2-TZVPP results. [b] Secondary “through-space” stabilization energy ΔE_{stab} evaluated as a difference between energies of the fully optimized silylium ions and the corresponding partially optimized structures with a fixed dip angle α^* in Fc unit B (and unit C where applicable) to 0.0° . [c] Data reported for the two minima found for $[\text{FcSiFc}_2]^+$.

benium system, and 2) a smaller atomic radius of silicon compared to the heavier congeners leading to somewhat more favorable interactions (see also Mayer bond orders in Table 2).

Isoelectronic neutral species containing boron or aluminum instead of the positively charged silicon atom display much smaller dip angles ($\alpha^* = 13.4^\circ$ and 32.5° , respectively) and lower stabilization energies. No ELF or ELI-D bonding attractors between iron and the electrophilic center are found in these species.^[42]

Among the silylium ions (Table 3), the largest ferrocenyl stabilization energies (ΔE_r and ΔE_{stab}) are generally found for the dialkyl-substituted species, the weakest for the diaryl analogues, particularly for those containing more than one Fc unit. The latter derivatives possess only one short $\text{Fe}\cdots\text{Si}$ distance ranging between about 2.54 and 2.63 Å, and one or two weaker $\text{Fc}\cdots\text{Si}^+$ interactions with $d(\text{Fc}\cdots\text{Si})$ varying from approximately 3.06 to 3.52 Å (Table 4).

For the monoferrocenyl-substituted systems, ΔE_r is about 30–60 kJ mol⁻¹ more negative than ΔE_{stab} . This provides a rough estimate of the stabilization due to the stronger inductive and mesomeric (+I/+M) effects of ferrocene relative to phenyl. In case of more than one Fc substituent (R and/or R' = Fc), the single primary donor-acceptor interaction with the smallest $\text{Fe}-\text{Si}$ distance is present on both sides of the isodesmic reaction (Scheme 1), and ΔE_r thus in-

cludes only the “pure” metallocene-backbone electronic effects and one or two weak (ca. 1.0–5.0 kJ mol⁻¹, Table 4) secondary “through-space” Fc···Si interactions. Incidentally, ΔE_r and ΔE_{stab} are very similar in these cases (Table 3).

To be able to better distinguish electronic from steric substituent effects, the computational study was further extended to systems combining diverse aryl and alkyl groups, and by introducing additional electron-donating/-withdrawing substituents into the *para* position of the silicon-bonded Ph substituent (this latter modification is not easily studied experimentally due to the likely occurrence of intermolecular donor–acceptor interactions). The data in Table 3 show that sterically less demanding substituents (Me in the alkyl series, Ph in the aryl series) lead to shorter Si···Fe and Si···C'_{ipso} distances and to larger dip angles, and thus to more effective interactions between the Fc moiety and the silylium center. On the other hand, sterically more demanding groups, such as *t*Bu or mesityl (Mes), diminish the interaction. Note that ΔE_{stab} for [FcSiMes₂]⁺ is about one order of magnitude lower than that for the dimethyl analogue.

In derivatives bearing two Fc substituents, secondary through-space interactions to the second Fc unit affect the resulting structure and NMR properties (see below). In general, differences between primary and secondary Fe···Si distances are much smaller in compounds with sterically less demanding groups, such as Me or Ph (Table 4). In the case of the silylium ion [FcSiFc₂]⁺ with three Fc units, two virtually isoenergetic minima were found. They differ in the orientation of the third Fc moiety (unit C) with respect to the FeCp₂ unit featuring the primary Fe···Si contact (Figure 4, the structure on the right is energetically favored by 0.9 kJ mol⁻¹) as well as in the distances between the silicon atom and the other atoms in question (Table 4). These structural differences result also in remarkably different ²⁹Si NMR chemical shifts calculated for the two stereoiso-

mers (Table 3; the Boltzmann-averaged value is used in this case for comparison with the experiment).

From Table 3 it is also evident that the stabilization energy is affected by both electronic and steric effects, and in most cases both act in the same direction (ΔE_{stab} decreases with increasing +I/+M effect and with increasing steric bulk of the alkyl/aryl substituents). This is demonstrated by plotting the stabilization energy against both electronic and steric Hammett–Taft parameters^[43] for the simplest case of two alkyl substituents (Figure 5).

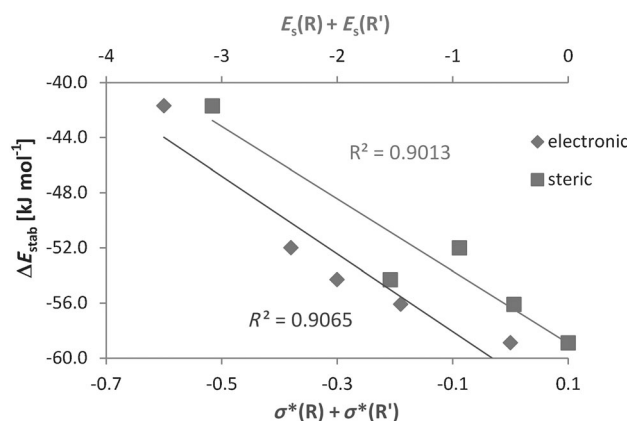


Figure 5. Dependence of ΔE_{stab} in a dialkyl series of ferrocene-stabilized silylium ions [FcSiR(R')]⁺ (R and R' = Me, *i*Pr, and *t*Bu) on electronic and steric parameters of R and R' substituents (expressed as a sum of their Hammett–Taft σ^* and E_s constants, respectively).

The situation becomes, however, more complicated when dealing with mixed alkyl/aryl systems. Here, silylium ions containing a bulkier *t*Bu group are somewhat more stabilized by a donor–acceptor interaction with the Fc group than those bearing a Me group (this is in contrast to the dia-

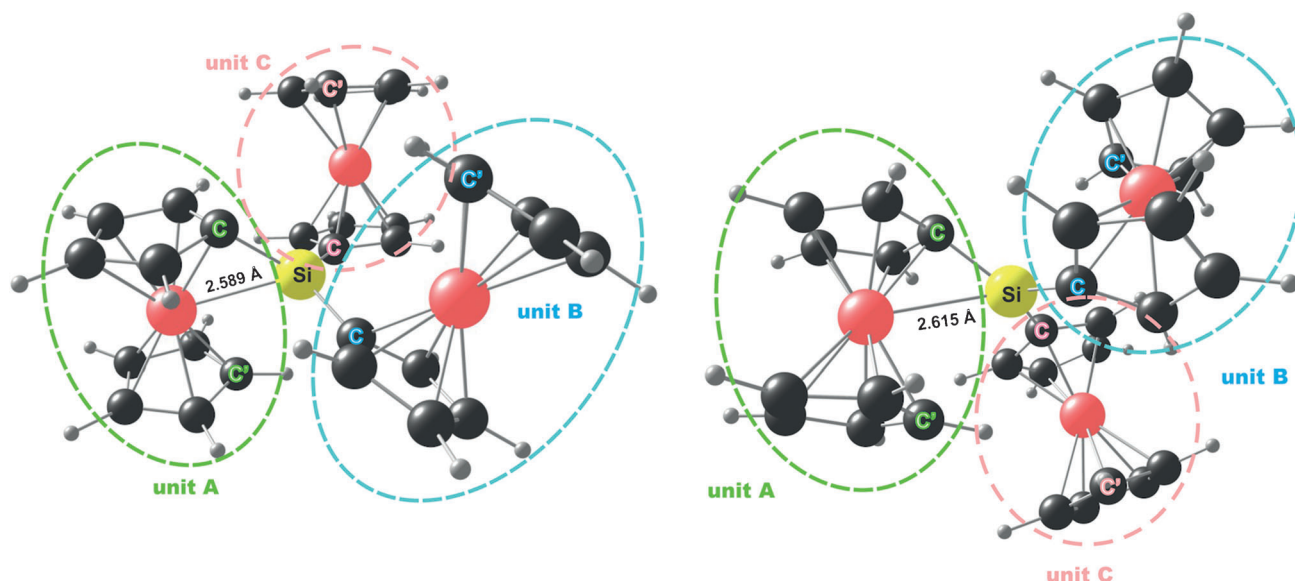


Figure 4. Schematic structures of the two virtually isoenergetic minima found for the silylium ion with three ferrocenyl units, [FcSiFc₂]⁺.

lkyl-substituted series but differences in ΔE_{stab} are less pronounced here). This behavior can be attributed to a much more pronounced twisting of the Ph ring from the SiC_3 plane in the *t*Bu-substituted derivatives due to steric congestion ($\tau=8.5^\circ$ in $[\text{FcSiPhMe}]^+$ whereas $\tau=67.7^\circ$ in $[\text{FcSiPh}(t\text{Bu})]^+$). This, in turn, causes the silylium center to have a higher tendency to attract electrons from ferrocene; see the somewhat shorter $\text{Si}\cdots\text{C}'_{\text{ipso}}$ distance in $[\text{FcSiPh}(t\text{Bu})]^+$ when compared to $[\text{FcSiPhMe}]^+$.

Analysis of ^{29}Si NMR chemical shifts: For the determination of the ^{29}Si NMR chemical shifts, a direct measurement was in most cases supported by a $^1\text{H},^{29}\text{Si}$ HMQC measurement due to a higher sensitivity for the latter technique. The ^{29}Si NMR chemical shifts of our new directly accessed silylium ions **9a–9k** (Table 1, column 8) as well as **9l** and **9m** obtained from substituent scrambling cover a broad range between $\delta=77.4$ and 120.9 ppm. Note that the ^{29}Si NMR chemical shifts in our ferrocenyl-substituted silylium ions do not alter upon changing the counterion.^[17] Interestingly, we see a strong dependence of the ^{29}Si NMR chemical shift on the choice of substituents at the silicon atom. In general, dialkyl substituted silylium ions **9a–9e** tend to show more high-frequency shifted signals ($\delta=110.7$ –120.9 ppm) than aryl-substituted cations **9f–9m** ($\delta=77.4$ –104.5 ppm), as supported by our DFT calculations (see below). This behavior is opposite to that observed for the hydride shifts of the silanes (Table 1, column 5), but overall the ^{29}Si NMR chemical shifts of the cations and the ^1H NMR chemical shifts of the corresponding silanes correlate only poorly (Figure S4 in the Supporting Information). This may be understood easily from the fact that the direct $\text{Fe}\cdots\text{Si}$ donor–acceptor interactions affect the former but not the latter. Moreover, ring current effects due to aromatic substituents can affect both shifts by up to about $\delta=1$ –2 ppm (see Figure S5 in the Supporting Information for a NICS analysis). Although this is an essentially negligible contribution to the ^{29}Si NMR chemical shifts, it is important for the ^1H NMR chemical shifts.

The agreement between measured and computed ^{29}Si NMR chemical shifts is excellent and consistent with a good quality of the PBE0-D3/def2-TZVPP optimized structures (Tables 1 and 3 as well as Figure 6). We note in passing that omission of the dispersion corrections from the optimizations results in structures with slightly longer $\text{Fe}\cdots\text{Si}$ and $\text{Si}\cdots\text{C}'_{\text{ipso}}$ distances (up to 0.04 Å), and consequently in inferior agreement with experimental NMR chemical shifts of the silylium ions (Table S2 and Figure S6 in the Supporting Information provide comparisons of different computational methods). The good quality of the computed chemical shifts allows us to further analyze the relations between ^{29}Si NMR chemical shifts and molecular and electronic structure, including also systems for which no experimental data are available.

NMR chemical shifts are still often interpreted as indicative of the atomic charge at the nucleus of interest, even though it is well known that the paramagnetic part of the Ramsey expression for the chemical shift may be influenced

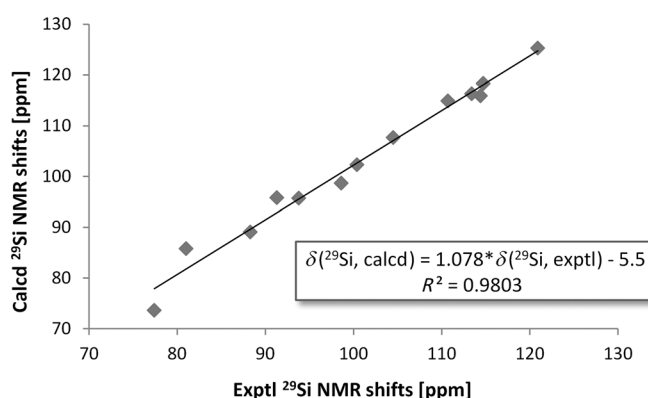


Figure 6. Correlation between experimental and calculated ^{29}Si NMR chemical shifts in a series of ferrocene-stabilized silylium ions (PBE0/IGLO-III//PBE0-D3/def2-TZVPP results with an IEF-PCM solvation model).

by several other factors. Therefore, such correlations with electron density (the electron-withdrawing/-donating character of the substituents) tend to be very limited.^[44] This is borne out also by the present results:^[45] although the dialkyl-substituted species exhibit generally more high-frequency shifted ^{29}Si NMR signals than those complexes with at least one aryl or a second Fc substituent (with the notable exception of $\text{R}=\text{Mes}$ and $\text{R}'=t\text{Bu}$; see below), the overall trends tend to be influenced in a complicated way by various factors (see also Figure S7 in the Supporting Information, showing a rather poor correlation, if any, between ^{29}Si NMR chemical shifts and Mulliken charges on the silylium center). This holds true despite the fact that, apparently, both steric and electronic substituent effects tend to work, at least to a certain extent, in the same direction (Figure 7). For example, the most downfield ^{29}Si NMR chemical shift within the studied ferrocene-stabilized silylium ions is found for $[\text{FcSi}(t\text{Bu})_2]^+$ (an even slightly more deshielded value is predicted for $[\text{FcSi}(t\text{Bu})\text{Mes}]^+$ and not for the dimethyl-substituted analogue (Table 3). This points already toward the importance of steric effects of R and R' substituents for

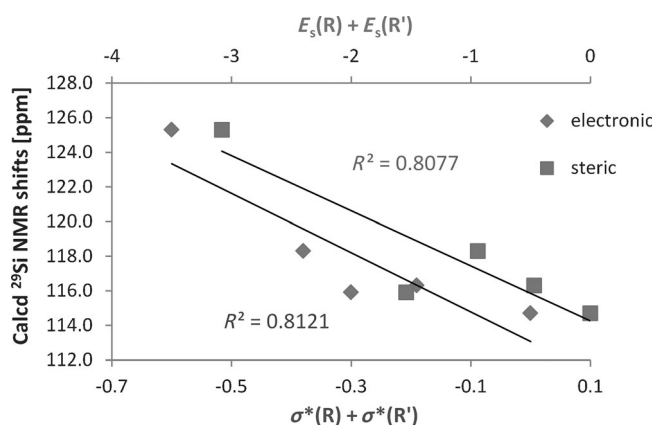


Figure 7. Dependence of calculated ^{29}Si NMR chemical shifts in a dialkyl series of ferrocene-stabilized silylium ions $[\text{FcSiR}(\text{R}')]^+$ (R and $\text{R}' = \text{Me}$, *i*Pr, and *t*Bu) on steric and electronic (Hammett–Taft) parameters.

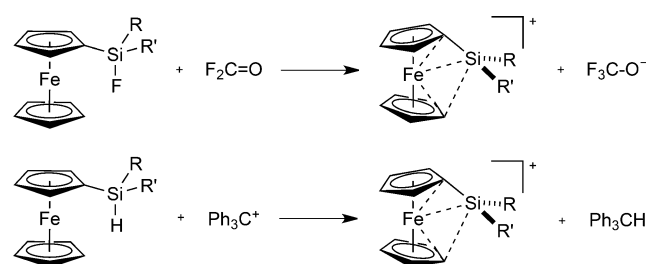
the stabilizing Fc...Si interaction (the large $d(\text{Fc}\cdots\text{Si})$ for $[\text{FcSi}(t\text{Bu})_2]^+$ in Table 3 and the discussion below).

Because of the diversity of the substituents attached to the silylium center and the various steric and electronic influences, we found it necessary to subdivide the series of cations into five subsets: 1) compounds with two alkyl substituents $[\text{FcSiAlk}_2]^+$, 2) compounds with one aryl and one alkyl substituent $[\text{FcSiArAlk}]^+$, 3) compounds with two aryl substituents $[\text{FcSiAr}_2]^+$, 4) compounds with two Ph substituents with varying *para*-substituent $[\text{FcSi}(p\text{-X-Ph})_2]^+$, and 5) compounds with more than one Fc unit $[\text{FcSiFcR}]^+$.

Using this division, a correlation of ^{29}Si NMR chemical shift and $d(\text{Fc}\cdots\text{Si})$ (or dip angle) becomes meaningful, and the established relationships may, in principle, be used for an indirect determination/estimation of the Fc...Si distances within the ferrocene-stabilized silylium ions using ^{29}Si NMR spectroscopy (Figure 8 and Figure S8 in the Supporting Information). Within a given subset, a shorter Fe...Si distance (larger dip angle) signals a more upfield ^{29}Si NMR chemical shift, consistent with a closer Fc...Si interaction shielding the silylium center. Systems with more than one Fc unit (blue diamonds) are a notable exception to this rule: here the secondary interactions with the second Fc unit reverse the trend! The longer the primary contact between the iron and silylium center becomes, the shorter the secondary interaction with the Fc unit B (Tables 3 and 4). In contrast to ΔE_{stab}

to significantly more deshielded $\delta(^{29}\text{Si})$ values. This effect is largest for systems with shorter secondary Fe...Si contacts ($\Delta\delta(^{29}\text{Si})=26.4$ ppm for $[\text{FcSiFcPh}]^+$ but only $\Delta\delta(^{29}\text{Si})=2.0$ ppm for $[\text{FcSiFc}(t\text{Bu})]^+$). An even larger deshielding effect (more than 120 ppm) is predicted upon complete cancellation of all "through-space" metallocene-silylium interactions (setting all dip angles within a given system to zero). Then we obtain ^{29}Si NMR chemical shifts comparable to or even more deshielded than that of the trimesityl silylium ion^[5] ($\delta(^{29}\text{Si})>200$ ppm; see Table S3 in the Supporting Information).

Lewis acidity: The strength of the Lewis acidity (electrophilicity) of silylium ions has been established on the basis of their fluoride ion affinities (FIA);^[46] see Scheme 2 for the associated isodesmic reaction). The FIA of a Lewis acid (A^+)



Scheme 2. Reactions used to evaluate the Lewis acidity.

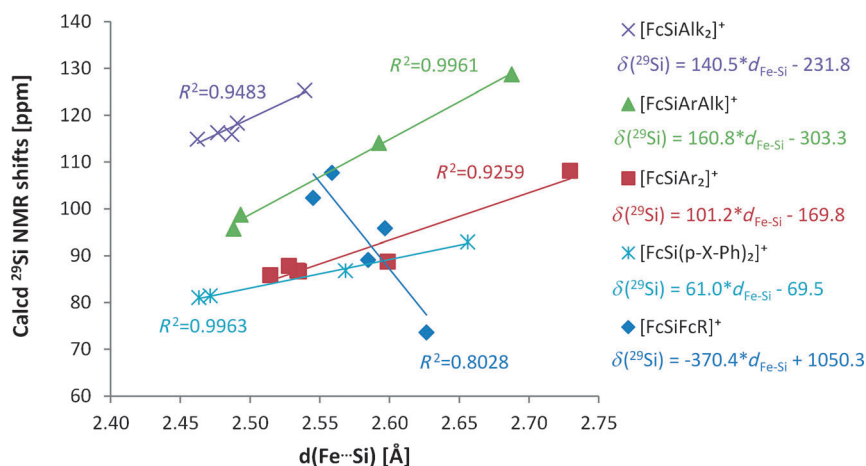


Figure 8. Correlation of computed ^{29}Si NMR chemical shifts with Fe...Si distance in the ferrocenyl-substituted silylium ions $[\text{FcSiR}(\text{R}')]^+$.

(see above), the secondary through-space interaction plays an important role for the ^{29}Si NMR chemical shifts and causes an additional shielding of the silylium center. This results, for example, in the most low-frequency ^{29}Si NMR chemical shift being observed for the silylium ion $[\text{FcSiFcPh}]^+$ ($\delta(^{29}\text{Si})=77.5$ ppm) with the shortest secondary Fe...Si contact. The effect of Lewis acid-base interactions on ^{29}Si NMR chemical shifts is also demonstrated in Table S3 in the Supporting Information. Switching off the secondary interaction by fixing the dip angle within unit B to 0.0° leads

is defined as the enthalpy change associated with the heterolytic cleavage of an A-F bond to give A^+ and F^- : the more positive the FIA, the stronger the Lewis acid.

In this study, FIA calculations were performed along the lines of Christie's method using F_2CO as a standard, which avoids the need to calculate free F^- in the gas phase.^[46,47] The FIA of each silicon cation was then calculated by adding the FIA of F_2CO , which is known experimentally (209 kJ mol⁻¹).^[46] Alternatively, we could have used the hydride

ion affinity (Scheme 2) with trityl cation as competing electrophile, closely related to the actual experimental generation of our silylium ions (see above). As we found an almost perfect correlation between these two quantities (Figure S9 in the Supporting Information), we will concentrate only on the FIAs in the following.

In general, all silylium ions studied here display enormous electrophilicity, larger than their carbenium congeners (for instance, the computed FIAs of $[\text{PhSiMe}_2]^+$ and $[\text{FcSiMe}_2]^+$ are 905 and 817 kJ mol⁻¹, respectively, whereas the FIAs in

the carbon cations $[\text{PhCMe}_2]^+$ and $[\text{FcCMe}_2]^+$ are 750 and 672 kJ mol^{-1} , respectively). The range of FIAs in the ferrocene-stabilized silylium ions (ca. 740–850 kJ mol^{-1} ; Table 3) is smaller than that in the corresponding phenyl series $[\text{PhSiR}(\text{R}')]^+$ (ca. 770–920 kJ mol^{-1} ; Table S4 in the Supporting Information), providing an indication that the Fc...Si interactions reduce the electrophilicity of the “free” silylium ion. However, we note also that this “Fc shielding effect” on the Lewis-acidity is much less dominant (e.g., compared to other substituent effects) than for the ^{29}Si NMR chemical shifts in which the ranges of the Fc- and Ph-substituted series are completely disjoint (Table 3 and Table S4 in the Supporting Information).

In both series, the highest Lewis acidity is found for derivatives bearing two alkyl substituents, and it decreases upon replacing alkyl by aryl substituents. The lowest electrophilicity is found for silylium ions with three aryl groups, especially when some of them include a ferrocene backbone (the more ferrocene units, the lower the Lewis acidity).

At first glance, one would expect that electronic +I effects of alkyl substituents lead to an increase of Lewis acidity in the order $t\text{Bu} < i\text{Pr} < \text{Me}$, as demonstrated, for example, for the all-alkyl series $[\text{MeSiR}_2]^+$ (Table S4 in Supporting Information). Surprisingly, however, the highest FIA in each of the ferrocenyl and phenyl series is found for derivatives with two $t\text{Bu}$ groups. In case of $[\text{FcSi}(t\text{Bu})_2]^+$, this can be attributed to a weakening of the Fc...Si interaction due to the steric bulk of the $t\text{Bu}$ groups ($d(\text{Fc}\cdots\text{Si})$ values in Table 3). On the other hand, in $[\text{PhSi}(t\text{Bu})_2]^+$ the steric repulsion between the $t\text{Bu}$ groups and *ortho* phenyl hydrogen atoms causes a pronounced twisting of the Ph ring out of the SiC_3 plane. The corresponding dihedral angle, τ , increases along the series $[\text{PhSiR}_2]^+$ ($\text{R} = \text{Me} < i\text{Pr} < t\text{Bu}$ as 0.0, 10.3, 31.0°), thereby also destabilizing the silicon cation and increasing its electrophilic character ($t\text{Bu}$ derivatives also exhibit somewhat longer Si–C bonds, that reduce the inductive +I effects to some extent). Note that closer inspection of the structures of our ferrocene-stabilized silylium ions did not reveal any C–H and/or C–C hyperconjugation effects, which play a role, for example, in the structure and NMR properties of more electron-deficient all-alkyl silicon cations.^[1e] The partly counterintuitive influence of the Fc...Si interactions in the ferrocenyl-substituted cations is best seen from plots of FIAs against ^{29}Si NMR chemical shifts while varying the *para*-substituent X on two Ph rings (Figure 9 and Table 3). In case of the $[\text{PhSi}(p\text{-X-Ph})_2]^+$ series, we find the expected correlation of larger FIA with more downfield ^{29}Si NMR chemical shifts upon going to more electron-withdrawing substituents, X (Figure 9a). Conversely, in the $[\text{FcSi}(p\text{-X-Ph})_2]^+$ series, the FIAs also increase but the ^{29}Si NMR chemical shifts actually decrease from X = NMe₂ to X = NO₂ (Figure 9b)! The latter trend can be understood from increased Fc...Si interactions for the more electron-withdrawing aryl groups (Fc...Si distances in Table 3). For this trend, the intramolecular Lewis acid–base interactions overcompensate the direct π donor (+M) effect of the aryl groups on the silylium center in case of the ^{29}Si NMR shifts

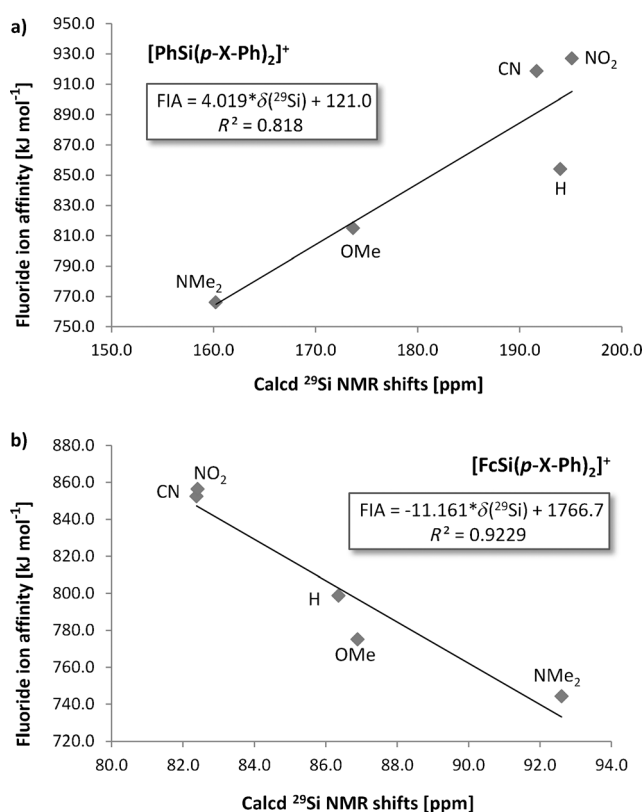


Figure 9. Correlation of computed fluoride ion affinities (FIAs) and ^{29}Si NMR chemical shifts in the: a) phenyl-silylium series $[\text{PhSi}(p\text{-X-Ph})_2]^+$, and b) ferrocenyl-silylium series $[\text{FcSi}(p\text{-X-Ph})_2]^+$ (X = NO₂, CN, H, OMe, NMe₂).

(note the overall much lower-frequency silicon shifts within a narrow range for the ferrocenyl systems compared to the phenyl analogues; Figure 9) but not in case of the FIAs.

These findings demonstrate already how different factors influence the ferrocenyl stabilization energies, the Lewis acidities, and the ^{29}Si NMR chemical shifts in a complicated fashion. Although steric and electronic effects go in the same direction for the ferrocenyl stabilization energies (Figure 5) and the ^{29}Si NMR chemical shifts of the ferrocenyl systems (Figure 7), these may work in opposite directions in other cases, for example, for the FIAs and chemical shifts of the “ferrocenyl-free” silylium ions (Figures S10 and S11 in the Supporting Information). For example, the Lewis acidity of the $[\text{PhSiR}(\text{R}')]^+$ series with $\text{R}, \text{R}' = \text{Me}, i\text{Pr}$ is primarily driven by electronic effects, whereas derivatives with $t\text{Bu}$ groups deviate due to dominant steric effects.

In the ferrocenyl-substituted systems, the steric and electronic effects on the FIAs also appear to work in opposite direction (Figure 10). This may explain why the various substituents can have such different effects on ^{29}Si NMR chemical shifts and Lewis acidity.

The extreme influence of Fc...Si interactions and steric effects on Lewis acidity may be seen best when comparing derivatives with Ph and Mes groups: the difference in FIA of $[\text{LSiPh}_2]^+$ and $[\text{LSiMes}_2]^+$ is about 12 kJ mol^{-1} in the ferrocenyl series (L = Fc; see Table 3) but approximately

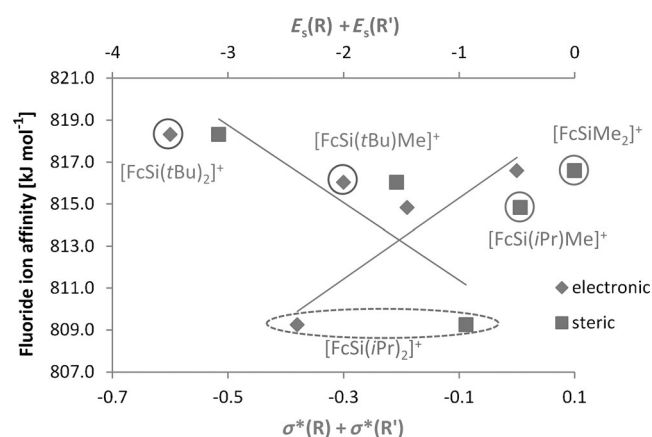


Figure 10. Dependence of fluoride ion affinities (FIAs) on steric and electronic (Hammett–Taft) parameters in a ferrocene-stabilized series $[\text{FcSiR}(\text{R}')]^+$ (R and $\text{R}' = \text{Me}$, $i\text{Pr}$, and $t\text{Bu}$).

33 kJ mol^{-1} in the phenyl series ($\text{L} = \text{Ph}$; see Table S4 in the Supporting Information). In the ferrocenyl series, the steric bulk of the Mes substituent diminishes the $\text{Fc}\cdots\text{Si}$ interaction and thus enhances the FIA, which approaches the value of $[\text{FcSiPh}_2]^+$. In contrast, in the ferrocenyl-free series, the stronger electron-donating effect of Mes compared to Ph substituents dominates, leading to the much lower electrophilicity of $[\text{PhSiMes}_2]^+$ as compared to the “free” triphenylsilylium ion.

We may extend our comparisons also to other experimentally known dialkyl-substituted silylium ions with rather different stabilization mechanisms (Figure 1). Table 5 shows

Table 5. Calculated fluoride ion affinities (FIAs) and ^{29}Si NMR chemical shifts in a series of dimethyl-substituted silylium ions and $[\text{Mes}_2\text{Si}]^+$.^[a,b]

Cmpd	FIA [kJ mol^{-1}]	$\delta(^{29}\text{Si})$ [ppm] ^[c]
$[\text{FcSiMe}_2]^+$ (this work)	816.6	113.7
1 ^[6]	807.8	84.7
2 ^[7]	796.6	77.4
3 ^[8]	811.3	81.5
4 ^[9a]	815.3	82.4
5 ^[9b]	756.8	61.0
6 ^[10]	680.7	17.3
Mes_2Si^+ ^[5]	800.0	229.5

[a] PBE0-D3/def2-TZVPP results in the gas-phase (see the Computational Methods for more detail). [b] See Figure 1 for the structures. [c] PBE0/IGLO-III/PBE0-D3/def2-TZVPP results in the gas-phase; see Figure 1 for the experimental values.

that the by far lowest Lewis acidity is found for compound **6**,^[10] which possesses a rigid structure and a cationic silicon center stabilized by two additional interactions with hydrogen atoms from the neighboring silyl groups. In contrast, the highest FIAs in this series are predicted for the hydrogen-bridged disilyl cation, **4**,^[9a] and $[\text{FcSiMe}_2]^+$.

For this series the FIAs correlate quite well with the ^{29}Si NMR chemical shifts (Figure 11). As demonstrated above, this is not the case for the ferrocenyl-substituted

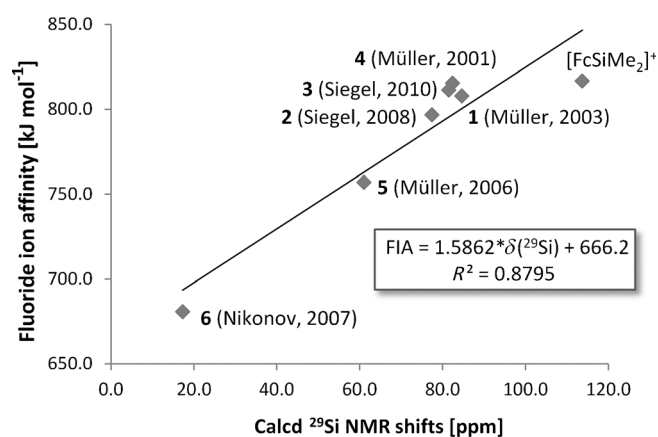


Figure 11. Correlation of calculated ^{29}Si NMR chemical shifts with FIAs in the series of dimethyl-substituted silylium ions (see Figure 1 for the structures).

series, due to the various steric and electronic factors working partly in opposite direction (Figures 9 and 10). Figure S12 in Supporting Information shows the overall very poor correlation between FIAs and ^{29}Si NMR chemical shifts, even after subdividing the ferrocenyl-substituted silylium ion series.

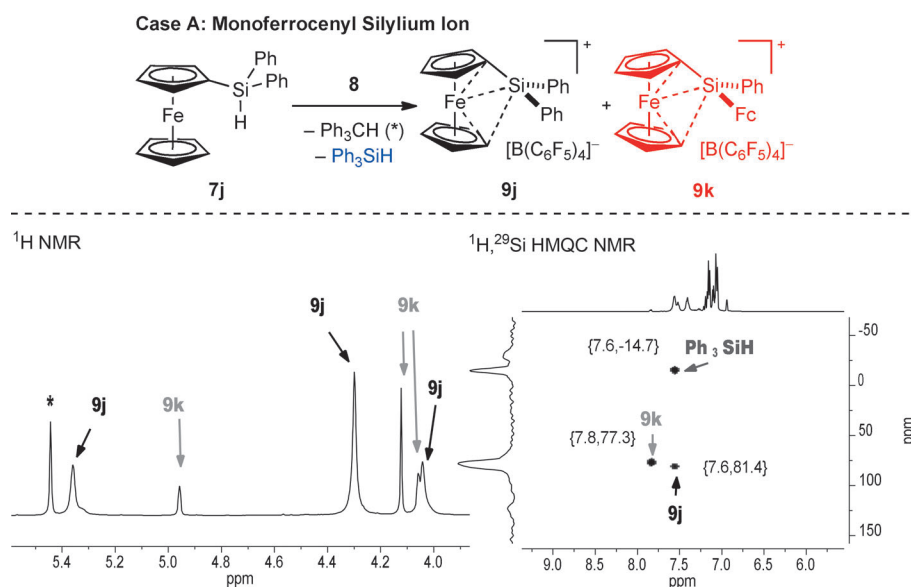
Furthermore, we have to note that both $[\text{FcSiMe}_2]^+$ and **4** are stronger Lewis acids than the trimesityl silylium ion $[\text{Mes}_3\text{Si}]^+$,^[5] which on the other hand, has a much more de-shielded silicon nucleus (Table 5).

Substituent scrambling: During our NMR spectroscopy studies of new ferrocene-stabilized silylium ions **9a–9k** we observed a second set of signals in the ^1H NMR spectra in some cases (note that NMR spectra were recorded 30 min and 6 h after mixing the reagents and the ratio between the expected and substituent-scrambled products did not change significantly during this period). This observation was accompanied by a second high-frequency shifted signal in the ^{29}Si NMR spectrum. When silane **7g** ($\text{R} = \text{Ph}$, $\text{R}' = \text{Me}$, Table 1, entry 7) was used as the precursor, even more cationic silicon species were generated. A careful analysis of these spectra revealed that more than one cationic silicon species produced by a scrambling of substituents was present in these cases (Table 1, column 9). Similar processes are not unprecedented in the literature.^[48,49] The group of Müller reported the exchange of substituents of silylium ions with silanes both in an intra-^[50] and intermolecular^[51] manner. Related substituent exchange reactions of silanes^[52] and skeletal rearrangements in polysilanes^[53] initiated by aluminum Lewis acids are also known.

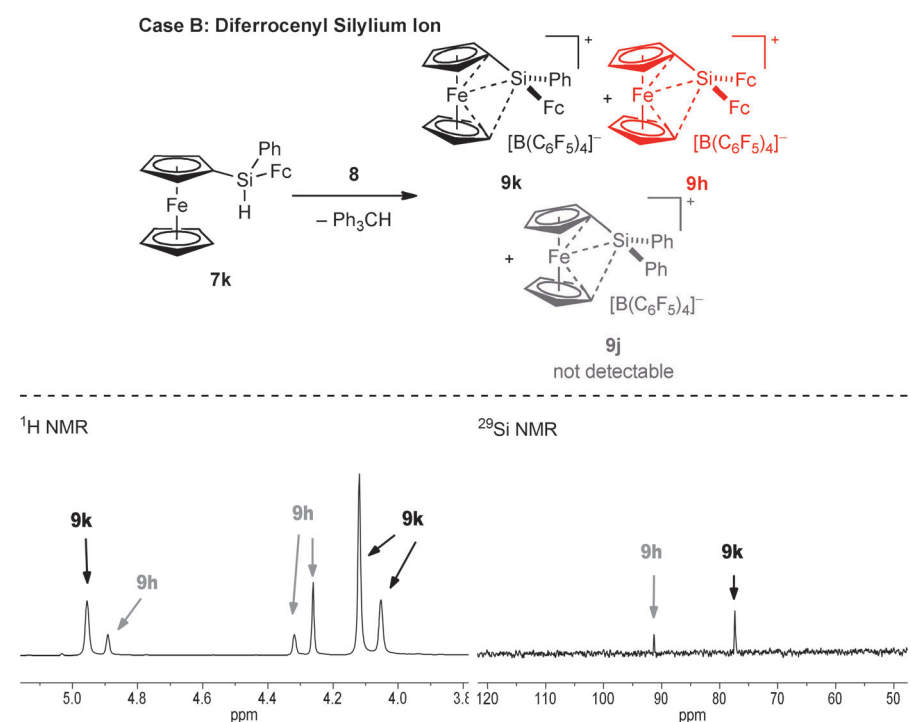
For our family of silylium ions, we noticed a substituent scrambling mainly when small substituents were attached to the silicon atom (Table 1, column 9). This is rationalized by the better accessibility of the silylium ion. We identified Me , Ph , and Fc groups as the only scrambling substituents, whereas a migration of $i\text{Pr}$ and $t\text{Bu}$ groups was not detected. This observation is in accord with the ability of the former groups to act as bridging groups between two silicon atoms

in a cationic species.^[54] Similar to Müller's report,^[51] sterically crowded silicon cations **9l** ($R = \text{Fc}$, $R' = t\text{Bu}$) and **9m** ($R = \text{Fc}$, $R' = i\text{Pr}$) were only accessible through substituent scrambling from cations **9c**, **9d** and **9f** (Table 1, entries 3, 4 and 6, respectively).

To further illustrate the observed product mixtures as a basis for a subsequent quantum-chemical analysis of the mechanism, we will focus on the discussion of two cases:



Scheme 3. Silylium ions **9j** and **9k** generated from silane **7j**. The relevant parts of the ^1H NMR (left) and $^1\text{H},^{29}\text{Si}$ HMQC NMR (right) spectra are shown as proof for substituent scrambling.



Scheme 4. Silylium ions **9k** and **9h** generated from silane **7k**. The relevant parts of the ^1H NMR (left) and ^{29}Si NMR (right) spectra are shown as proof for substituent scrambling.

silane **7j** (Table 1, entry 10) as an example of a monoferrocenylsilane (Scheme 3, case A) and silane **7k** (Table 1, entry 11) as an example of a diferrocenylsilane (Scheme 4, case B). The treatment of monoferrocenylsilane **7j** with $[\text{Ph}_3\text{C}]^+[\text{B}(\text{C}_6\text{F}_5)_4]^-$ (**8**) affords the primary hydride abstraction product **9j** and silylium ion **9k** by the exchange of a Ph and a Fc substituent (Scheme 3, upper). Both products were clearly identified in the ^1H and $^1\text{H},^{29}\text{Si}$ HMQC NMR spectra (Scheme 3, lower).

The ^1H NMR spectrum shows two sets of signals consisting of three signals each for the protons of the upper and the lower Cp rings. In addition to the two silicon cations **9j** ($\delta = 81.4$ ppm) and **9k** ($\delta = 77.3$ ppm) a third silicon species ($\delta = -14.7$ ppm) was detected in the $^1\text{H},^{29}\text{Si}$ HMQC NMR, assigned as Ph_3SiH . A further hydride abstraction reaction from Ph_3SiH with still unreacted trityl cation is not observed at short reaction times and room temperature.

In a second example, diferrocenylsilane **7k** is treated with $[\text{Ph}_3\text{C}]^+[\text{B}(\text{C}_6\text{F}_5)_4]^-$ (**8**) yielding the direct hydride abstraction product **9k** and, by exchange of a Ph and a Fc group, silylium ion **9h** (Scheme 4, upper). Both silylium ions **9k** and **9h** were identified by their two sets of signals in the ^1H NMR spectrum and their two signals in the ^{29}Si NMR spectrum (Scheme 4, lower). Another expected ferrocene-stabilized silicon cation **9j** derived from substituent scrambling was not detected although treatment with unreacted trityl salt **8** ought to be possible as it would also be a ferrocene-stabilized silylium ion. Presumably, silylium ion **9h** is easier to detect in the ^1H NMR spectrum (Scheme 4, lower left) due to three identical Fc substituents. Signals of traces of **9j** in the ^1H NMR spectrum might either be hidden under signals of the other silicon cations **9k** and **9h** or were not detected.

To elucidate the mechanism and energetic feasibility of the

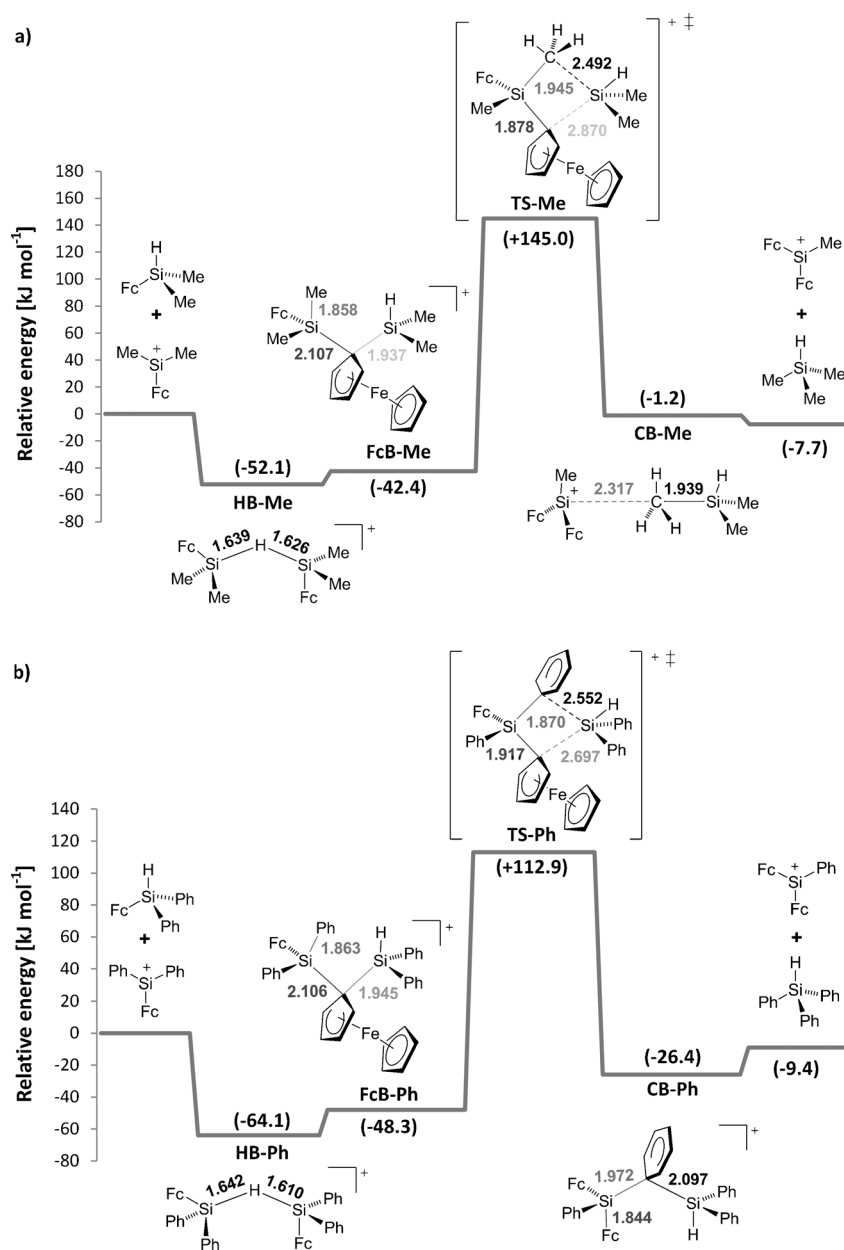


Figure 12. Computed (PBE0-D3/def2-TZVPP/COSMO) reaction mechanisms for substituent scrambling in two selected ferrocenyl-substituted silylium ions in reactions with the silicon hydride precursors. a) Methyl-group transfer in $[\text{FcSiMe}_2]^+$ (**9e**); b) phenyl-group transfer in $[\text{FcSiPh}_2]^+$ (**9j**). Relative energies [kJ mol^{-1}] with respect to the energy of reactants are given in parentheses.

substituent-scrambling process, DFT calculations were performed (see Figure 12 for the PBE0-D3/def2-TZVPP/COSMO results and Figure S13 in the Supporting Information for corresponding gas-phase results). Note that counterion effects were neglected and the computed energies thus probably provide only a rough estimate of the barriers. We chose $[\text{FcSiMe}_2]^+$ (**9e**, Table 1, entry 5) as an example for a methyl-transfer and $[\text{FcSiPh}_2]^+$ (**9j**, Table 1, entry 10) for a phenyl-transfer process. Treatment of these silylium ions with the corresponding silicon hydride precursor **7e** and **7j**, respectively, provides in both instances the hydride-bridged

dimers **HB-Me** or **HB-Ph** as the lowest-energy minimum (however, the free energies of these species are slightly above those of the reactants due to entropic reasons).^[4] Yet, ferrocenyl-bridged species **FcB-Me** or **FcB-Ph** are energetically accessible and present the opportunity for the methyl shift (Figure 12a) or phenyl shift (Figure 12b), respectively. The transition states **TS-Me** and **TS-Ph** may be considered asymmetrical and “early” regarding the formation of the new Si–C bond. Nevertheless, we observe a concerted substituent-transfer process starting from the ferrocenyl-bridged intermediates **FcB-Me** or **FcB-Ph**. The ferrocenyl bridge opens simultaneously with the partial formation of the new Si–C bond, leading to the methyl- or phenyl-bridged intermediates **CB-Me** and **CB-Ph**, respectively. These open finally to the respective substituent scrambling products. The transition states are computed to lie at 145 kJ mol^{-1} , relative to the reactants, in the methyl transfer case, and at about 110 kJ mol^{-1} in the phenyl transfer case. The overall reaction energies are slightly exothermic by about 10 kJ mol^{-1} . The computed barriers are somewhat higher than those reported by Müller et al. for an intramolecular exchange of substituents in disilyl cations with a rigid naphthalene-1,8-diyl backbone ($80\text{--}90 \text{ kJ mol}^{-1}$),^[50] but they are still in a range indicating feasible

substituent scrambling processes in both cases, with a somewhat faster reaction for the phenyl transfer.

Conclusion

We have recently reported $[\text{FcSi}(t\text{Bu})\text{Me}]^+$ as an example of a ferrocene-stabilized silylium ion in which donor–acceptor Fe–Si interactions contribute to a “taming” of its Lewis acidity and reactivity, providing an interesting starting point for the design of tailor-made Lewis-acid catalysts. Here we

extend this new class of compounds to a series of more than ten members with various substitution patterns, all characterized by detailed NMR spectroscopy studies in solution, covering a large range of ^{29}Si NMR chemical shifts ($\delta = 77.4\text{--}120.9$ ppm). In parallel, an even larger set of such ferrocenyl-substituted silylium ions has been examined by detailed quantum-chemical analyses of molecular and electronic structure, intramolecular donor–acceptor stabilization energies, Lewis-acidity measures, as well as ^{29}Si NMR chemical shifts.

The direct stabilizing $\text{Fe}\cdots\text{Si}$ interactions in the ferrocenyl-substituted silylium ions are apparent from various electronic-structure analyses, for example, bond orders, ELF, or ELI-D plots, and are manifested also in the magnitude of the dip angle and $\text{Fe}\cdots\text{Si}$ distances. Notably, computations show that this interaction is more pronounced for silylium ions than for lighter or heavier group 14 homologues, and much stronger than for neutral group 13 species. However, steric and electronic properties of the substituents at the silylium center combine in a subtle way to influence the Lewis acidity (e.g., fluoride ion affinities) and the spectroscopic parameters (e.g., ^{29}Si NMR chemical shifts) of the ferrocenyl-substituted silylium ions, leading to partly non-intuitive trends. For example, although in simpler model silylium ions more electron-withdrawing substituents (e.g., in the *para* position of a phenyl group) increase both the Lewis acidity and the ^{29}Si NMR chemical shifts, enhanced $\text{Fe}\cdots\text{Si}$ interactions in ferrocenyl-substituted cations reverse the trend for the silicon shifts (but not for fluoride ion affinities). Matters become even more involved when more than one ferrocenyl substituent is present, as both a strong primary $\text{Fe}\cdots\text{Si}$ interaction and weaker through-space secondary $\text{Fc}\cdots\text{Si}$ interaction(s) have to be considered. Correlations between ^{29}Si NMR chemical shifts and Lewis-acidity measures are thus restricted to subsets of complexes and ^{29}Si NMR chemical shifts should be generally taken with caution when evaluating the electrophilic character of the silylium ions. Explicit quantum-chemical computations of these properties, nevertheless, provide substantial predictive power and appreciable insight and can help to design ferrocene-substituted silylium ions with specific catalytic activity. Furthermore, a reasonable correlation of ^{29}Si NMR chemical shift and $\text{Fe}\cdots\text{Si}$ distances found for a subset of complexes may be used for an indirect determination of $\text{Fe}\cdots\text{Si}$ “bond” lengths within the ferrocene-stabilized silylium ions using ^{29}Si NMR spectroscopy.

Systematic NMR spectroscopy studies have revealed substituent exchange processes in several of the less sterically hindered ferrocenyl-substituted silylium ions, due to reaction of the initially formed cation with unreacted silane starting material. This “substituent scrambling” involves mostly the transfer of smaller Me and Ph substituents and leads to the formation of new silylium ions with different substitution patterns, albeit not quantitatively. The feasibility of a concerted bimolecular mechanism for these processes, based on ferrocenyl-bridged intermediates, is supported by explicit

quantum-chemical calculations of thermochemistry and barriers for two representative cases.

Experimental Section

All reactions were performed in flame-dried glassware using an MBraun glove box ($\text{O}_2 < 0.5$ ppm, $\text{H}_2\text{O} < 0.5$ ppm) or conventional Schlenk techniques under a static pressure of argon or nitrogen. Liquids and solutions were transferred with syringes. THF was dried over potassium. Technical grade solvents for extraction or chromatography (cyclohexane and *tert*-butyl methyl ether) were distilled prior to use. $1,2\text{-Cl}_2\text{C}_6\text{D}_4$ (Amar Chemicals or Eurisotop) was dried over CaH_2 prior to use and stored over molecular sieves in a glove box. C_6D_6 (Eurisotop) was used without further purification and was stored over molecular sieves. Ferrocene (Alfa Aesar) was used without further purification. Chlorosilanes were either purchased from the indicated commercial suppliers and used without further purification [*t*Bu₂HSiCl (Fluka), *i*Pr₂HSiCl (ABCR), Me₂HSiCl (Sigma–Aldrich), MePhSiCl₂ (Merck), HSiCl₃ (Sigma–Aldrich), MeHSiCl₂ (Sigma–Aldrich), Ph₂HSiCl (ABCR), PhHSiCl₂ (Alfa Aesar)] or prepared in analogy to reported procedures [*t*BuMeHSiCl from MeHSiCl₂ and *t*BuLi,^[6a] Me*i*PrHSiCl from MeHSiCl₂ and *i*PrMgCl,^[55] *t*BuPhHSiCl from PhHSiCl₂ and *t*BuLi^[56]]. $[\text{Ph}_3\text{C}]^+[\text{B}(\text{C}_6\text{F}_5)_4]^-$ (**8**)^[57] was prepared according to a reported procedure. Analytical thin layer chromatography (TLC) was performed on silica gel 60 F254 glass plates by Merck. Flash column chromatography was performed on silica gel 60 (40–63 μm , 230–400 mesh, ASTM) by Merck using the indicated solvents. ^1H , ^{11}B , ^{13}C , ^{19}F and ^{29}Si NMR spectra were recorded in C_6D_6 or $1,2\text{-Cl}_2\text{C}_6\text{D}_4$ on Bruker AV300, Bruker AV400, and Varian INOVA 500 instruments (Westfälische Wilhelms-Universität Münster) and Bruker AV400 and AV500 instruments (Technische Universität Berlin). Chemical shifts are reported in parts per million (ppm) and are referenced to the residual solvent resonance as the internal standard ($\text{C}_6\text{D}_6\text{H}$: $\delta = 7.16$ ppm for ^1H NMR and C_6D_6 : $\delta = 128.1$ ppm for ^{13}C NMR; $1,2\text{-Cl}_2\text{C}_6\text{D}_3\text{H}$: $\delta = 6.94$ and 7.20 ppm for ^1H NMR and $1,2\text{-Cl}_2\text{C}_6\text{D}_4$: $\delta = 127.1$, 130.1 and 132.5 ppm for ^{13}C NMR). Data are reported as follows: chemical shift, multiplicity (brs = broad singlet, s = singlet, d = doublet, t = triplet, q = quartet, sept = septet, br m = broad multiplet, m = multiplet, m_c = centrosymmetric multiplet), coupling constants (Hz) and integration. ^1H , ^{29}Si HMQC NMR spectra were measured with a coupling constant of 7.0 Hz for the $^3J_{\text{H,Si}}$ coupling. The peak intensities in the ^1H , ^{29}Si HMQC NMR spectra cannot be correlated to the amount of compound. Gas liquid chromatography (GLC) was performed on a Shimadzu GC-17A gas chromatograph equipped with a SE-54 capillary column (30 m \times 0.32 mm, 0.25 μm film thickness) by CS-Chromatographie Service using the following program: N₂ carrier gas, injection temperature 240 °C, detector temperature 300 °C, flow rate: 1.74 mL min⁻¹; temperature program: start temperature 40 °C, heating rate 10 °C min⁻¹, end temperature 280 °C for 10 min. Infrared (IR) spectra were recorded on a Varian 3100 FT-IR spectrometer (Westfälische Wilhelms-Universität Münster) and an Agilent Technologies Cary 630 FT-IR spectrometer (Technische Universität Berlin), both equipped with an ATR unit and are reported in wavenumbers [cm⁻¹]. Melting points (m.p.) were determined with a Stuart Scientific SMP20 melting point apparatus and are not corrected. Mass spectrometry (MS) was obtained from the Analytical Facilities at the Organisch-Chemisches Institut, Westfälische Wilhelms-Universität Münster and at the Institut für Chemie, Technische Universität Berlin.

General procedure for the preparation of ferrocene-stabilized silicon cations **9 (GP 2):** In a glove box, a solution of a ferrocenylsilane (1.00 equiv) in $1,2\text{-Cl}_2\text{C}_6\text{D}_4$ (0.3 mL) was added to a suspension of $[\text{Ph}_3\text{C}]^+[\text{B}(\text{C}_6\text{F}_5)_4]^-$ (**8**, 1.00 equiv) in $1,2\text{-Cl}_2\text{C}_6\text{D}_4$ (0.2 mL) in an 8 mL vial equipped with a magnetic stir bar. The resulting red-brown solution was stirred for 1 min, transferred to an NMR tube, and directly subjected to NMR spectroscopic analysis.

Di-*tert*-butylferrocenylsilylium tetrakis(pentafluorophenyl)borate (9a**):** This was prepared from di-*tert*-butylferrocenylsilane (**7a**, 32.5 mg, 99.1 μmol , 1.00 equiv) and $[\text{Ph}_3\text{C}]^+[\text{B}(\text{C}_6\text{F}_5)_4]^-$ (**8**, 91.4 mg, 99.1 μmol ,

1.00 equiv) according to GP 2. ^1H NMR (500 MHz, 1,2- $\text{Cl}_2\text{C}_6\text{D}_4$): δ = 1.11 (s, 18H), 3.89 (brs, 2H), 4.36 (brs, 5H), 5.26 ppm (brs, 2H); ^{13}C NMR (125 MHz, 1,2- $\text{Cl}_2\text{C}_6\text{D}_4$): δ = 28.3, 30.7, 65.3, 73.5, 82.3, 86.5, 124.5 (brm), 136.6 (d, $J_{\text{C,F}}$ = 245 Hz), 138.5 (d, $J_{\text{C,F}}$ = 243 Hz), 148.6 ppm (d, $J_{\text{C,F}}$ = 242 Hz); ^{11}B NMR (126 MHz, 1,2- $\text{Cl}_2\text{C}_6\text{D}_4$): δ = -16.2 ppm; ^{19}F NMR (470 MHz, 1,2- $\text{Cl}_2\text{C}_6\text{D}_4$): δ = -166.0, -162.1, -131.8 ppm; $^1\text{H},^{29}\text{Si}$ HMOC NMR (99 MHz, 1,2- $\text{Cl}_2\text{C}_6\text{D}_4$): δ = 120.3 ppm; ^{29}Si NMR (99 MHz, 1,2- $\text{Cl}_2\text{C}_6\text{D}_4$): δ = 120.9 ppm.

Ferrocenyldi-*iso*-propylsilylium tetrakis(pentafluorophenyl)borate (9b): This was prepared from ferrocenyldi-*iso*-propylsilane (**7b**, 25.2 mg, 83.9 μmol , 1.00 equiv) and $[\text{Ph}_3\text{C}]^+[\text{B}(\text{C}_6\text{F}_5)_4]^-$ (**8**, 77.4 mg, 83.9 μmol , 1.00 equiv) according to GP 2. ^1H NMR (500 MHz, 1,2- $\text{Cl}_2\text{C}_6\text{D}_4$): δ = 1.16 (m, 12H), 1.38–1.47 (m, 2H), 3.76 (brs, 2H), 4.33 (brs, 5H), 5.21 ppm (brs, 2H); ^{13}C NMR (125 MHz, 1,2- $\text{Cl}_2\text{C}_6\text{D}_4$): δ = 17.8, 18.4, 20.7, 65.7, 73.4, 80.9, 86.6, 124.5 (brm), 136.6 (d, $J_{\text{C,F}}$ = 245 Hz), 138.5 (d, $J_{\text{C,F}}$ = 245 Hz), 148.6 ppm (d, $J_{\text{C,F}}$ = 238 Hz); ^{11}B NMR (76 MHz, 1,2- $\text{Cl}_2\text{C}_6\text{D}_4$): δ = -16.2 ppm; ^{19}F NMR (282 MHz, 1,2- $\text{Cl}_2\text{C}_6\text{D}_4$): δ = -166.1, -162.0, -131.8 ppm; $^1\text{H},^{29}\text{Si}$ HMOC NMR (99 MHz, 1,2- $\text{Cl}_2\text{C}_6\text{D}_4$): δ = 114.1 ppm; ^{29}Si NMR (99 MHz, 1,2- $\text{Cl}_2\text{C}_6\text{D}_4$): δ = 114.7 ppm.

***tert*-Butylferrocenylmethylsilylium tetrakis(pentafluorophenyl)borate (9c):** This was prepared from *tert*-butylferrocenylmethylsilane (**7c**, 23.3 mg, 81.5 μmol , 1.00 equiv) and $[\text{Ph}_3\text{C}]^+[\text{B}(\text{C}_6\text{F}_5)_4]^-$ (**8**, 75.1 mg, 81.5 μmol , 1.00 equiv) according to GP 2 along with traces of silylium ion **9l**. ^1H NMR (300 MHz, 1,2- $\text{Cl}_2\text{C}_6\text{D}_4$): δ = 0.71 (s, 3H), 1.07 (s, 9H), 3.58 (brs, 1H), 4.93 (brs, 1H), 4.27 (brs, 5H), 5.21 ppm (brs, 2H); ^{13}C NMR (125 MHz, 1,2- $\text{Cl}_2\text{C}_6\text{D}_4$): δ = -4.4, 24.7, 27.7, 64.7, 73.8, 81.0, 81.4, 86.4, 87.1, 124.5 (brm), 136.6 (d, $J_{\text{C,F}}$ = 242 Hz), 138.6 (d, $J_{\text{C,F}}$ = 242 Hz), 148.6 ppm (d, $J_{\text{C,F}}$ = 242 Hz); ^{11}B NMR (160 MHz, 1,2- $\text{Cl}_2\text{C}_6\text{D}_4$): δ = -16.4 ppm; ^{19}F NMR (470 MHz, 1,2- $\text{Cl}_2\text{C}_6\text{D}_4$): δ = -166.1, -162.2, -132.0 ppm; $^1\text{H},^{29}\text{Si}$ HMOC NMR (99 MHz, 1,2- $\text{Cl}_2\text{C}_6\text{D}_4$): δ = 113.9 ppm; ^{29}Si NMR (60 MHz, 1,2- $\text{Cl}_2\text{C}_6\text{D}_4$): δ = 114.4 ppm.

Ferrocenylmethyl-*iso*-propylsilylium tetrakis(pentafluorophenyl)borate (9d): This was prepared from ferrocenylmethyl-*iso*-propylsilane (**7d**, 21.4 mg, 78.6 μmol , 1.00 equiv) and $[\text{Ph}_3\text{C}]^+[\text{B}(\text{C}_6\text{F}_5)_4]^-$ (**8**, 72.5 mg, 78.6 μmol , 1.00 equiv) according to GP 2 along with silylium ion **9m**. ^1H NMR (500 MHz, 1,2- $\text{Cl}_2\text{C}_6\text{D}_4$): δ = 0.74 (s, 3H), 1.13 (m, 6H), 1.41 (sept, J = 7.6 Hz, 1H), 3.67 (brs, 1H), 3.82 (brs, 1H), 4.28 (brs, 5H), 5.22 ppm (brs, 2H); ^{13}C NMR (125 MHz, 1,2- $\text{Cl}_2\text{C}_6\text{D}_4$): δ = -5.4, 17.4, 19.2, 19.9, 65.7, 73.9, 80.6, 80.8, 86.8, 86.9, 124.3 (brm), 136.5 (d, $J_{\text{C,F}}$ = 244 Hz), 138.5 (d, $J_{\text{C,F}}$ = 244 Hz), 148.5 ppm (d, $J_{\text{C,F}}$ = 243 Hz); ^{11}B NMR (126 MHz, 1,2- $\text{Cl}_2\text{C}_6\text{D}_4$): δ = -16.3 ppm; ^{19}F NMR (470 MHz, 1,2- $\text{Cl}_2\text{C}_6\text{D}_4$): δ = -166.2, -162.1, -132.1 ppm; $^1\text{H},^{29}\text{Si}$ HMOC NMR (99 MHz, 1,2- $\text{Cl}_2\text{C}_6\text{D}_4$): δ = 113.5 ppm; ^{29}Si NMR (99 MHz, 1,2- $\text{Cl}_2\text{C}_6\text{D}_4$): δ = 113.4 ppm.

Ferrocenyldimethylsilylium tetrakis(pentafluorophenyl)borate (9e): This was prepared from ferrocenyldimethylsilane (**7e**, 19.7 mg, 80.7 μmol , 1.00 equiv) and $[\text{Ph}_3\text{C}]^+[\text{B}(\text{C}_6\text{F}_5)_4]^-$ (**8**, 74.4 mg, 80.7 μmol , 1.00 equiv) according to GP 2 along with silylium ion **9i**. ^1H NMR (500 MHz, 1,2- $\text{Cl}_2\text{C}_6\text{D}_4$): δ = 0.82 (brs, 6H), 3.68 (brs, 2H), 4.21 (brs, 5H), 5.18 ppm (brs, 2H); ^{13}C NMR (125 MHz, 1,2- $\text{Cl}_2\text{C}_6\text{D}_4$): δ = -1.6, 66.4, 74.4, 80.3, 86.8, 124.3 (brm), 136.5 (d, $J_{\text{C,F}}$ = 246 Hz), 138.4 (d, $J_{\text{C,F}}$ = 245 Hz), 148.4 ppm (d, $J_{\text{C,F}}$ = 242 Hz); ^{11}B NMR (126 MHz, 1,2- $\text{Cl}_2\text{C}_6\text{D}_4$): δ = -16.5 ppm; ^{19}F NMR (470 MHz, 1,2- $\text{Cl}_2\text{C}_6\text{D}_4$): δ = -166.3, -162.1, -132.2 ppm; $^1\text{H},^{29}\text{Si}$ HMOC NMR (99 MHz, 1,2- $\text{Cl}_2\text{C}_6\text{D}_4$): δ = 111.0 ppm; ^{29}Si NMR (99 MHz, 1,2- $\text{Cl}_2\text{C}_6\text{D}_4$): δ = 110.7 ppm.

***tert*-Butylferrocenylphenylsilylium tetrakis(pentafluorophenyl)borate (9f):** Prepared from *tert*-butylferrocenylphenylsilane (**7f**, 41.1 mg, 118 μmol , 1.00 equiv) and $[\text{Ph}_3\text{C}]^+[\text{B}(\text{C}_6\text{F}_5)_4]^-$ (**8**, 109 mg, 118 μmol , 1.00 equiv) according to GP 2 along with traces of silylium ion **9l**. ^1H NMR (300 MHz, 1,2- $\text{Cl}_2\text{C}_6\text{D}_4$): δ = 1.13 (s, 9H), 3.44 (brs, 1H), 4.06 (brs, 1H), 4.35 (brs, 5H), 5.18 (brs, 1H), 5.24 (brs, 1H), 7.36–7.39 (m, 2H), 7.45–7.50 ppm (m, 3H); ^{13}C NMR (75 MHz, 1,2- $\text{Cl}_2\text{C}_6\text{D}_4$): δ = 25.9, 28.2, 64.5, 73.8, 81.7, 83.0, 86.6, 87.4, 124.6 (brm), 126.3, 129.8, 133.7, 134.1, 136.7 (d, $J_{\text{C,F}}$ = 245 Hz), 138.6 (d, $J_{\text{C,F}}$ = 238 Hz), 148.7 ppm (d, $J_{\text{C,F}}$ = 245 Hz); ^{11}B NMR (76 MHz, 1,2- $\text{Cl}_2\text{C}_6\text{D}_4$): δ = -16.3 ppm; ^{19}F NMR (282 MHz, 1,2- $\text{Cl}_2\text{C}_6\text{D}_4$): δ = -166.1, -162.1, -132.0 ppm; $^1\text{H},^{29}\text{Si}$ HMOC NMR (99 MHz, 1,2- $\text{Cl}_2\text{C}_6\text{D}_4$): δ = 98.8 ppm; ^{29}Si NMR (59 MHz, 1,2- $\text{Cl}_2\text{C}_6\text{D}_4$): δ = 98.6 ppm.

Ferrocenylmethylphenylsilylium tetrakis(pentafluorophenyl)borate (9g): This was prepared from ferrocenylmethylphenylsilane (**7g**, 25.3 mg, 82.6 μmol , 1.00 equiv) and $[\text{Ph}_3\text{C}]^+[\text{B}(\text{C}_6\text{F}_5)_4]^-$ (**8**, 76.2 mg, 82.6 μmol , 1.00 equiv) according to GP 2 along with silylium ions **9e**, **9i**, **9j** and traces of **9k**. Due to the complex mixture of silylium ions only some characteristic signals in the ^1H NMR spectrum could be assigned. The ^{13}C NMR spectrum was not interpretable. ^1H NMR (500 MHz, 1,2- $\text{Cl}_2\text{C}_6\text{D}_4$): δ = 1.07 (brs), 5.29 (brs), 7.26–7.59 ppm (m); ^{11}B NMR (126 MHz, 1,2- $\text{Cl}_2\text{C}_6\text{D}_4$): δ = -16.7 ppm; ^{19}F NMR (470 MHz, 1,2- $\text{Cl}_2\text{C}_6\text{D}_4$): δ = -166.6, -162.4, -132.6 ppm; ^{29}Si NMR (99 MHz, 1,2- $\text{Cl}_2\text{C}_6\text{D}_4$): δ = 93.8 ppm.

Triferrocenylsilylium tetrakis(pentafluorophenyl)borate (9h): This was prepared from triferrocenylsilane (**7h**, 52.4 mg, 89.7 μmol , 1.00 equiv) and $[\text{Ph}_3\text{C}]^+[\text{B}(\text{C}_6\text{F}_5)_4]^-$ (**8**, 82.7 mg, 89.7 μmol , 1.00 equiv) according to GP 2. ^1H NMR (500 MHz, 1,2- $\text{Cl}_2\text{C}_6\text{D}_4$): δ = 4.25 (brs, 15H), 4.31 (brs, 6H), 4.88 ppm (brs, 6H); ^{13}C NMR (125 MHz, 1,2- $\text{Cl}_2\text{C}_6\text{D}_4$): δ = 52.8, 72.2, 76.5, 79.1, 124.5 (brm), 136.6 (d, $J_{\text{C,F}}$ = 247 Hz), 138.6 (d, $J_{\text{C,F}}$ = 245 Hz), 148.6 ppm (d, $J_{\text{C,F}}$ = 245 Hz); ^{11}B NMR (126 MHz, 1,2- $\text{Cl}_2\text{C}_6\text{D}_4$): δ = -16.2 ppm; ^{19}F NMR (470 MHz, 1,2- $\text{Cl}_2\text{C}_6\text{D}_4$): δ = -165.9, -162.0, -131.8 ppm; $^1\text{H},^{29}\text{Si}$ HMOC NMR (99 MHz, 1,2- $\text{Cl}_2\text{C}_6\text{D}_4$): δ = 91.3 ppm; ^{29}Si NMR (99 MHz, 1,2- $\text{Cl}_2\text{C}_6\text{D}_4$): δ = 91.3 ppm.

Diferrocenylmethylsilylium tetrakis(pentafluorophenyl)borate (9i): This was prepared from diferrocenylmethylsilane (**7i**, 35.2 mg, 85.0 μmol , 1.00 equiv) and $[\text{Ph}_3\text{C}]^+[\text{B}(\text{C}_6\text{F}_5)_4]^-$ (**8**, 78.4 mg, 85.0 μmol , 1.00 equiv) according to GP 2 along with traces of silylium ion **9h**. ^1H NMR (500 MHz, 1,2- $\text{Cl}_2\text{C}_6\text{D}_4$): δ = 1.17 (s, 3H), 3.98 (brs, 4H), 4.16 (brs, 10H), 4.92 ppm (brs, 4H); ^{13}C NMR (125 MHz, 1,2- $\text{Cl}_2\text{C}_6\text{D}_4$): δ = -3.6, 52.7, 72.8, 76.2, 81.7, 124.3 (brm), 136.5 (d, $J_{\text{C,F}}$ = 246 Hz), 138.4 (d, $J_{\text{C,F}}$ = 243 Hz), 148.5 ppm (d, $J_{\text{C,F}}$ = 242 Hz); ^{11}B NMR (126 MHz, 1,2- $\text{Cl}_2\text{C}_6\text{D}_4$): δ = -16.5 ppm; ^{19}F NMR (470 MHz, 1,2- $\text{Cl}_2\text{C}_6\text{D}_4$): δ = -166.2, -162.3, -132.1 ppm; $^1\text{H},^{29}\text{Si}$ HMOC NMR (99 MHz, 1,2- $\text{Cl}_2\text{C}_6\text{D}_4$): δ = 88.5 ppm; ^{29}Si NMR (99 MHz, 1,2- $\text{Cl}_2\text{C}_6\text{D}_4$): δ = 88.3 ppm.

Ferrocenyldiphenylsilylium tetrakis(pentafluorophenyl)borate (9j): This was prepared from ferrocenyldiphenylsilane (**7j**, 29.4 mg, 79.9 μmol , 1.00 equiv) and $[\text{Ph}_3\text{C}]^+[\text{B}(\text{C}_6\text{F}_5)_4]^-$ (**8**, 73.7 mg, 79.9 μmol , 1.00 equiv) according to GP 2 along with silylium ion **9k**. ^1H NMR (500 MHz, 1,2- $\text{Cl}_2\text{C}_6\text{D}_4$): δ = 4.04 (brs, 2H), 4.30 (brs, 5H), 5.36 (brs, 2H), 7.39–7.42 (m, 4H), 7.51–7.60 ppm (m, 6H); ^{13}C NMR (125 MHz, 1,2- $\text{Cl}_2\text{C}_6\text{D}_4$): δ = 62.4, 75.5, 81.4, 87.4, 124.4 (brm), 124.6, 129.9, 135.8, 136.5 (d, $J_{\text{C,F}}$ = 244 Hz), 136.6, 138.5 (d, $J_{\text{C,F}}$ = 244 Hz), 148.5 ppm (d, $J_{\text{C,F}}$ = 241 Hz); ^{11}B NMR (126 MHz, 1,2- $\text{Cl}_2\text{C}_6\text{D}_4$): δ = -16.5 ppm; ^{19}F NMR (470 MHz, 1,2- $\text{Cl}_2\text{C}_6\text{D}_4$): δ = -166.4, -162.3, -132.3 ppm; $^1\text{H},^{29}\text{Si}$ HMOC NMR (99 MHz, 1,2- $\text{Cl}_2\text{C}_6\text{D}_4$): δ = 81.4 ppm; ^{29}Si NMR (99 MHz, 1,2- $\text{Cl}_2\text{C}_6\text{D}_4$): δ = 81.0 ppm.

Diferrocenylphenylsilylium tetrakis(pentafluorophenyl)borate (9k): This was prepared from diferrocenylphenylsilane (**7k**, 37.6 mg, 79.0 μmol , 1.00 equiv) and $[\text{Ph}_3\text{C}]^+[\text{B}(\text{C}_6\text{F}_5)_4]^-$ (**8**, 72.8 mg, 79.0 μmol , 1.00 equiv) according to GP 2 along with silylium ion **9h**. ^1H NMR (500 MHz, 1,2- $\text{Cl}_2\text{C}_6\text{D}_4$): δ = 4.05 (brs, 4H), 4.12 (brs, 10H), 4.95 (brs, 4H), 7.52 (dd, J = 7.6 Hz, J = 7.6 Hz, 2H), 7.60 (t, J = 7.7 Hz, 1H), 7.84 ppm (d, J = 7.4 Hz, 2H); ^{13}C NMR (125 MHz, 1,2- $\text{Cl}_2\text{C}_6\text{D}_4$): δ = 51.4, 73.1, 76.9, 81.8, 124.6 (brm), 125.0, 130.1, 134.4, 134.5, 136.7 (d, $J_{\text{C,F}}$ = 244 Hz), 138.6 (d, $J_{\text{C,F}}$ = 242 Hz), 148.7 ppm (d, $J_{\text{C,F}}$ = 242 Hz); ^{11}B NMR (126 MHz, 1,2- $\text{Cl}_2\text{C}_6\text{D}_4$): δ = -16.1 ppm; ^{19}F NMR (470 MHz, 1,2- $\text{Cl}_2\text{C}_6\text{D}_4$): δ = -165.8, -161.9, -131.7 ppm; $^1\text{H},^{29}\text{Si}$ HMOC NMR (99 MHz, 1,2- $\text{Cl}_2\text{C}_6\text{D}_4$): δ = 77.5 ppm; ^{29}Si NMR (99 MHz, 1,2- $\text{Cl}_2\text{C}_6\text{D}_4$): δ = 77.4 ppm.

***tert*-Butyldiferrocenylsilylium tetrakis(pentafluorophenyl)borate (9l):** ^1H NMR (300 MHz, 1,2- $\text{Cl}_2\text{C}_6\text{D}_4$): δ = 1.34 (s, 9H), 4.06 (brs, 4H), 4.16 (s, 10H), 4.91 ppm (brs, 4H); ^{13}C NMR (125 MHz, 1,2- $\text{Cl}_2\text{C}_6\text{D}_4$): δ = 25.3, 29.7, 55.0, 72.7, 78.0, 80.9, 124.5 (brm), 136.6 (d, $J_{\text{C,F}}$ = 242 Hz), 138.6 (d, $J_{\text{C,F}}$ = 242 Hz), 148.6 ppm (d, $J_{\text{C,F}}$ = 242 Hz); ^{11}B NMR (160 MHz, 1,2- $\text{Cl}_2\text{C}_6\text{D}_4$): δ = -16.4 ppm; ^{19}F NMR (470 MHz, 1,2- $\text{Cl}_2\text{C}_6\text{D}_4$): δ = -166.1, -162.2, -132.0 ppm; $^1\text{H},^{29}\text{Si}$ HMOC NMR (99 MHz, 1,2- $\text{Cl}_2\text{C}_6\text{D}_4$): δ = 104.5 ppm.

Diferrocenyl-*iso*-propylsilylium tetrakis(pentafluorophenyl)borate (9m): ^1H NMR (500 MHz, 1,2- $\text{Cl}_2\text{C}_6\text{D}_4$): δ = 1.38–1.44 (m, 6H), 1.83 (sept, J = 7.4 Hz, 1H), 3.99 (brs, 4H), 4.17 (s, 10H), 4.92 ppm (s, 4H); ^{13}C NMR (125 MHz, 1,2- $\text{Cl}_2\text{C}_6\text{D}_4$): δ = 16.8, 17.5, 53.9, 72.5, 76.7, 81.2, 124.3 (brm),

136.5 (d, $J_{\text{CF}}=244$ Hz), 138.5 (d, $J_{\text{CF}}=244$ Hz), 148.5 ppm (d, $J_{\text{CF}}=243$ Hz); ^{13}C NMR (160 MHz, 1,2- $\text{Cl}_2\text{C}_6\text{D}_4$): $\delta=-16.3$ ppm; ^{19}F NMR (470 MHz, 1,2- $\text{Cl}_2\text{C}_6\text{D}_4$): $\delta=-166.2$, -162.1 , -132.1 ppm; ^1H , ^{29}Si HMQC NMR (99 MHz, 1,2- $\text{Cl}_2\text{C}_6\text{D}_4$): $\delta=100.4$ ppm.

Acknowledgements

This research was (in part) supported by the Cluster of Excellence "Unifying Concepts in Catalysis" (UniCat; EXC 314, 2012–2017) and the Deutsche Forschungsgemeinschaft (Oe 249/9-1). K.M. also thanks the Studienstiftung des Deutschen Volkes for a predoctoral fellowship (2009–2012), and P.H. gratefully acknowledges the Alexander von Humboldt Foundation for a research fellowship. K.M. is a member of the International Research Training Group Münster-Nagoya (GRK 1143 of the Deutsche Forschungsgemeinschaft). M.O. is indebted to the Einstein Foundation (Berlin) for an endowed professorship.

- [1] a) A. Schulz, A. Villinger, *Angew. Chem.* **2012**, *124*, 4602–4604; *Angew. Chem. Int. Ed.* **2012**, *51*, 4526–4528; b) H. F. T. Klare, M. Oestreich, *Dalton Trans.* **2010**, 39, 9176–9184; c) T. Müller, *Adv. Organomet. Chem.* **2005**, *53*, 155–215; d) J. B. Lambert, Y. Zhao, S. M. Zhang, *J. Phys. Org. Chem.* **2001**, *14*, 370–379; e) C. A. Reed, *Acc. Chem. Res.* **1998**, *31*, 325–332.
- [2] a) J. B. Lambert, S. Zhang, C. L. Stern, J. C. Huffman, *Science* **1993**, *260*, 1917–1918; b) M. Farooq Ibad, P. Langer, A. Schulz, A. Villinger, *J. Am. Chem. Soc.* **2011**, *133*, 21016–21027.
- [3] C. A. Reed, Z. Xie, R. Bau, A. Benesi, *Science* **1993**, *262*, 402–404.
- [4] S. P. Hoffmann, T. Kato, F. S. Tham, C. A. Reed, *Chem. Commun.* **2006**, 767–769.
- [5] a) J. B. Lambert, Y. Zhao, *Angew. Chem.* **1997**, *109*, 389–391; *Angew. Chem. Int. Ed. Engl.* **1997**, *36*, 400–401; b) K.-C. Kim, C. A. Reed, D. W. Elliot, L. J. Mueller, F. Tham, L. Lin, J. B. Lambert, *Science* **2002**, *297*, 825–827.
- [6] T. Müller, C. Bauch, M. Ostermeier, M. Bolte, N. Auner, *J. Am. Chem. Soc.* **2003**, *125*, 2158–2168.
- [7] S. Duttwyler, Q.-Q. Do, A. Linden, K. K. Baldrige, J. S. Siegel, *Angew. Chem.* **2008**, *120*, 1743–1746; *Angew. Chem. Int. Ed.* **2008**, *47*, 1719–1722.
- [8] P. Romanato, S. Duttwyler, A. Linden, K. K. Baldrige, J. S. Siegel, *J. Am. Chem. Soc.* **2010**, *132*, 7828–7829.
- [9] a) T. Müller, *Angew. Chem.* **2001**, *113*, 3123–3126; *Angew. Chem. Int. Ed.* **2001**, *40*, 3033–3036; b) R. Panisch, M. Bolte, T. Müller, *J. Am. Chem. Soc.* **2006**, *128*, 9676–9682.
- [10] A. Y. Khalimon, Z. H. Lin, R. Simionescu, S. F. Vyboishchikov, G. I. Nikonov, *Angew. Chem.* **2007**, *119*, 4614–4617; *Angew. Chem. Int. Ed.* **2007**, *46*, 4530–4533.
- [11] V. Y. Lee, A. Sekiguchi, *Acc. Chem. Res.* **2007**, *40*, 410–419.
- [12] a) C. Bleiholder, F. Rominger, R. Gleiter, *Organometallics* **2009**, *28*, 1014–1017; for a review, see: b) R. Gleiter, C. Bleiholder, F. Rominger, *Organometallics* **2007**, *26*, 4850–4859; for a seminal article, see: c) M. Cais, *Organomet. Chem. Rev.* **1966**, *1*, 435–454.
- [13] a) T. Renk, W. Ruf, W. Siebert, *J. Organomet. Chem.* **1976**, *120*, 1–25; b) A. Appel, F. Jäkle, T. Priermeier, R. Schmid, M. Wagner, *Organometallics* **1996**, *15*, 1188–1194; c) B. E. Carpenter, W. E. Piers, M. Parvez, G. P. A. Yap, S. J. Rettig, *Can. J. Chem.* **2001**, *79*, 857–867; d) M. Scheibitz, M. Bolte, J. W. Bats, H.-W. Lerner, I. Nowik, R. H. Herber, A. Krapp, M. Lein, M. C. Holthausen, M. Wagner, *Chem. Eur. J.* **2005**, *11*, 584–603.
- [14] J. Y. Corey, D. Gust, K. Mislow, *J. Organomet. Chem.* **1975**, *101*, C7–C8.
- [15] a) M. J. MacLachlan, S. C. Bourke, A. J. Lough, I. Manners, *J. Am. Chem. Soc.* **2000**, *122*, 2126–2127; b) S. C. Bourke, M. J. MacLachlan, A. J. Lough, I. Manners, *Chem. Eur. J.* **2005**, *11*, 1989–2000.
- [16] a) H. F. T. Klare, K. Bergander, M. Oestreich, *Angew. Chem.* **2009**, *121*, 9241–9243; *Angew. Chem. Int. Ed.* **2009**, *48*, 9077–9079; b) R. K. Schmidt, K. Mütter, C. Mück-Lichtenfeld, S. Grimme, M. Oestreich, *J. Am. Chem. Soc.* **2012**, *134*, 4421–4428.
- [17] K. Mütter, R. Fröhlich, C. Mück-Lichtenfeld, S. Grimme, M. Oestreich, *J. Am. Chem. Soc.* **2011**, *133*, 12442–12444.
- [18] U. Behrens, *J. Organomet. Chem.* **1979**, *182*, 89–98.
- [19] a) J. P. Perdew, K. Burke, M. Ernzerhof, *Phys. Rev. Lett.* **1996**, *77*, 3865–3868; b) C. Adamo, V. Barone, *Chem. Phys. Lett.* **1998**, *298*, 113–119.
- [20] S. Grimme, J. Antony, S. Ehrlich, H. Krieg, *J. Chem. Phys.* **2010**, *132*, 154104.
- [21] F. Weigend, R. Ahlrichs, *Phys. Chem. Chem. Phys.* **2005**, *7*, 3297–3305.
- [22] J. Tao, J. P. Perdew, V. N. Staroverov, G. E. Scuseria, *Phys. Rev. Lett.* **2003**, *91*, 146401.
- [23] TURBOMOLE, version 6.3.1, a Development of University of Karlsruhe and Forschungszentrum Karlsruhe, GmbH, **1989–2007**, TURBOMOLE GmbH since **2007**; available from <http://www.turbomole.com>.
- [24] Gaussian 09, Revision A.02, M. J. Frisch, G. W. Trucks, H. B. Schlegel, G. E. Scuseria, M. A. Robb, J. R. Cheeseman, G. Scalmani, V. Barone, B. Mennucci, G. A. Petersson, H. Nakatsuji, M. Caricato, X. Li, H. P. Hratchian, A. F. Izmaylov, J. Bloino, G. Zheng, J. L. Sonnenberg, M. Hada, M. Ehara, K. Toyota, R. Fukuda, J. Hasegawa, M. Ishida, T. Nakajima, Y. Honda, O. Kitao, H. Nakai, T. Vreven, J. A. Montgomery, Jr., J. E. Peralta, F. Ogliaro, M. Bearpark, J. J. Heyd, E. Brothers, K. N. Kudin, V. N. Staroverov, R. Kobayashi, J. Normand, K. Raghavachari, A. Rendell, J. C. Burant, S. S. Iyengar, J. Tomasi, M. Cossi, N. Rega, J. M. Millam, M. Klene, J. E. Knox, J. B. Cross, V. Bakken, C. Adamo, J. Jaramillo, R. Gomperts, R. E. Stratmann, O. Yazyev, A. J. Austin, R. Cammi, C. Pomelli, J. W. Ochterski, R. L. Martin, K. Morokuma, V. G. Zakrzewski, G. A. Voth, P. Salvador, J. J. Dannenberg, S. Dapprich, A. D. Daniels, Ö. Farkas, J. B. Foresman, J. V. Ortiz, J. Cioslowski, D. J. Fox, Gaussian, Inc., Wallingford CT, **2009**.
- [25] K. Wolinski, J. F. Hinton, P. Pulay, *J. Am. Chem. Soc.* **1990**, *112*, 8251–8260.
- [26] M. Munzarova, M. Kaupp, *J. Phys. Chem. A* **1999**, *103*, 9966–9983.
- [27] W. Kutzelnigg, U. Fleischer, M. Schindler, in *NMR Basic Principles and Progress*, Vol. 23 (Eds.: P. Diehl, E. Fluck, H. Günther, R. Kosfeld, J. Seelig), Springer, Heidelberg, **1991**, pp. 165–262.
- [28] J. Tomasi, B. Mennucci, R. Cammi, *Chem. Rev.* **2005**, *105*, 2999–3093.
- [29] A. Klamt, G. Schüürmann, *J. Chem. Soc. Perkin Trans. 2* **1993**, 799–805.
- [30] a) A. D. Becke, K. E. Edgecombe, *J. Chem. Phys.* **1990**, *92*, 5397–5403; b) A. Savin, O. Jepsen, J. Flad, O. K. Andersen, H. Preuss, H. G. von Schnering, *Angew. Chem.* **1992**, *104*, 185–186; *Angew. Chem. Int. Ed. Engl.* **1992**, *31*, 185–187; c) M. Kohout, A. Savin, *Int. J. Quantum Chem.* **1996**, *60*, 875–882.
- [31] a) M. Kohout, *Int. J. Quantum Chem.* **2004**, *97*, 651–658; b) M. Kohout, K. Pernal, F. R. Wagner, Y. Grin, *Theor. Chem. Acc.* **2004**, *112*, 453–459; Wagner, Y. Grin, *Theor. Chem. Acc.* **2004**, *112*, 453–459.
- [32] M. Kohout, DGrid, version 4.6, Radebeul, **2011**.
- [33] a) I. Mayer, *Chem. Phys. Lett.* **1983**, *97*, 270–274; b) I. Mayer, *Chem. Phys. Lett.* **1985**, *117*, 396.
- [34] I. Mayer, BORDER, version 1.0, Chemical Research Center, Hungarian Academy of Sciences, Budapest, **2005**; available from <http://occam.chemres.hu/programs>.
- [35] Paraview, version 3.8, Kitware Inc., Clifton Park, New York, USA, **2010**; available from: <http://www.paraview.org>.
- [36] J. Y. Corey, *J. Am. Chem. Soc.* **1975**, *97*, 3237–3238.
- [37] R. Sanders, U. T. Mueller-Westerhoff, *J. Organomet. Chem.* **1996**, *512*, 219–224.
- [38] O. Riant, G. Argouarch, D. Guillauneux, O. Samuel, H. B. Kagan, *J. Org. Chem.* **1998**, *63*, 3511–3514.
- [39] Experimental details on the preparation of all ferrocenylsilanes **7a–7k** can be found in the Supporting Information.

- [40] For a comparable family of different terphenyl substituted silylium ions, see: a) ref. [7]; b) ref. [8]; c) P. Romanato, S. Duttwyler, A. Linden, K. K. Baldrige, J. S. Siegel, *J. Am. Chem. Soc.* **2011**, *133*, 11844–11846; d) C. Gerdes, W. Saak, D. Haase, T. Müller, *J. Am. Chem. Soc.* **2013**, *135*, 10353–10361.
- [41] P. Pykkö, M. Atsumi, *Chem. Eur. J.* **2009**, *15*, 186–197.
- [42] For a discussion of bonding in ferrocenylboranes in terms of molecular orbitals and an energy partitioning analysis, see ref. [13d].
- [43] C. Hansch, A. Leo, R. W. Taft, *Chem. Rev.* **1991**, *91*, 165–195.
- [44] M. Kaupp, in *Calculation of NMR and EPR Parameters: Theory and Applications* (Eds.: M. Kaupp, M. Bühl, V. G. Malkin), Wiley-VCH, Weinheim, **2004**, pp. 293–306.
- [45] The ²⁹Si NMR chemical shift of cationic silicon species is often viewed as a measurement of their degree of silylium ion character: G. A. Olah, L. D. Field, *Organometallics* **1982**, *1*, 1485–1487.
- [46] a) T. E. Mallouk, G. L. Rosenthal, G. Müller, R. Brusasco, N. Bartlett, *Inorg. Chem.* **1984**, *23*, 3167–3173; b) K. O. Christe, D. A. Dixon, D. McLemore, W. W. Wilson, J. A. Sheehy, J. A. Boatz, *J. Fluorine Chem.* **2000**, *101*, 151–153.
- [47] For some recent applications of FIA as a measure of Lewis acidity, see for example: a) J. M. Slattery, S. Hussein, *Dalton Trans.* **2012**, *41*, 1808–1815; b) T. A. Engesser, P. Hrobárik, N. Trapp, P. Eiden, H. Scherer, M. Kaupp, I. Krossing, *ChemPlusChem* **2012**, *77*, 643–651.
- [48] For similar rearrangements during solvolysis reactions of silyl halides, see: a) C. Eaborn, D. A. R. Happer, K. D. Safa, D. R. M. Walton, *J. Organomet. Chem.* **1978**, *157*, C50–C52; b) C. Eaborn, D. A. R. Happer, S. P. Hopper, K. D. Safa, *J. Organomet. Chem.* **1980**, *188*, 179–192; c) C. Eaborn, P. D. Lickiss, S. T. Najim, W. A. Stańczyk, *J. Chem. Soc. Chem. Commun.* **1987**, 1461–1462.
- [49] For a related 1,3-methyl shift in a polysilyl silylium ion, see: M. Nakamoto, T. Fukawa, A. Sekiguchi, *Chem. Lett.* **2004**, *33*, 38–39.
- [50] N. Lühmann, H. Hirao, S. Shaik, T. Müller, *Organometallics* **2011**, *30*, 4087–4096.
- [51] a) A. Schäfer, M. Reißmann, A. Schäfer, W. Saak, D. Haase, T. Müller, *Angew. Chem.* **2011**, *123*, 12845–12848; *Angew. Chem. Int. Ed.* **2011**, *50*, 12636–12638; b) A. Schäfer, M. Reißmann, S. Jung, A. Schäfer, W. Saak, E. Brendler, T. Müller, *Organometallics* **2013**, *32*, 4713–4722.
- [52] a) J. L. Speier, R. E. Zimmerman, *J. Am. Chem. Soc.* **1955**, *77*, 6395–6396; b) M. Khandelwal, R. J. Wehmschulte, *Angew. Chem.* **2012**, *124*, 7435–7439; *Angew. Chem. Int. Ed.* **2012**, *51*, 7323–7326.
- [53] a) M. Ishikawa, J. Iyoda, H. Ikeda, K. Kotake, T. Hashimoto, M. Kumada, *J. Am. Chem. Soc.* **1981**, *103*, 4845–4850; b) M. Ishikawa, M. Watanabe, J. Iyoda, H. Ikeda, M. Kumada, *Organometallics* **1982**, *1*, 317–322; c) T. A. Blinka, R. West, *Organometallics* **1986**, *5*, 128–133; d) J. Fischer, J. Baumgartner, C. Marschner, *Science* **2005**, *310*, 825; e) H. Wagner, J. Baumgartner, T. Müller, C. Marschner, *J. Am. Chem. Soc.* **2009**, *131*, 5022–5023.
- [54] For examples of bissilylated arenium ions, see: a) R. Meyer, K. Werner, T. Müller, *Chem. Eur. J.* **2002**, *8*, 1163–1172; b) N. Choi, P. D. Lickiss, M. McPartlin, P. C. Masangane, G. L. Veneziani, *Chem. Commun.* **2005**, 6023–6025; c) R. Panisch, M. Bolte, T. Müller, *Organometallics* **2007**, *26*, 3524–3529.
- [55] R. D. Holmes-Smith, S. R. Stobart, *J. Am. Chem. Soc.* **1980**, *102*, 382–384.
- [56] C. M. DiBlasi, D. E. Macks, D. S. Tan, *Org. Lett.* **2005**, *7*, 1777–1780.
- [57] a) C. Wang, G. Erker, G. Kehr, K. Wedeking, R. Fröhlich, *Organometallics* **2005**, *24*, 4760–4773; b) J. B. Lambert, L. Lin, S. Keinan, *Org. Biomol. Chem.* **2003**, *1*, 2559–2565.

Please note: Minor changes have been made to this manuscript since its publication in *Chemistry – A European Journal* Early View. The Editor.

Received: July 23, 2013
Published online: October 21, 2013